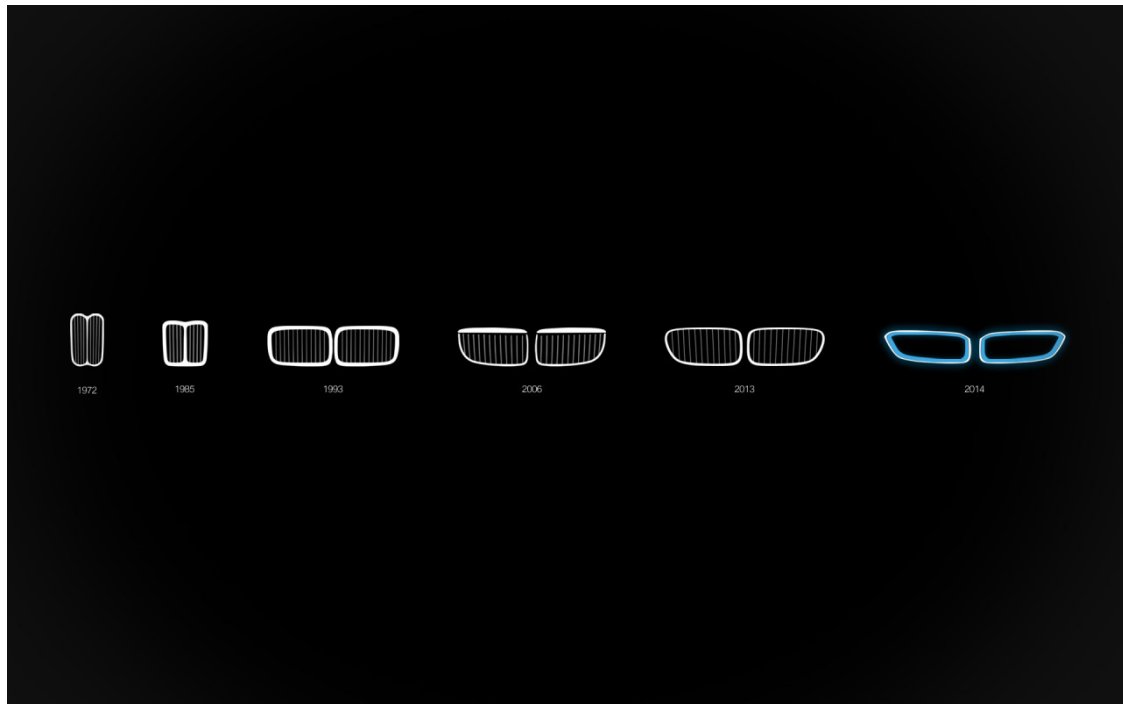




CHALMERS
UNIVERSITY OF TECHNOLOGY



Cell Level Power Electronics for Better Battery Management System

Master's thesis in Electric Power Engineering

SRI VISHNU GORANTLA NARAYANA MURTHY



MASTER'S THESIS 2016

Cell Level Power Electronics for Better Battery Management System

Sri Vishnu Gorantla Narayana Murthy



CHALMERS
UNIVERSITY OF TECHNOLOGY

Department of Energy and Environment
Division of Electric Power Engineering
CHALMERS UNIVERSITY OF TECHNOLOGY
Gothenburg, Sweden 2016

Cell Level Power Electronics for Better Battery Management System
SRI VISHNU GORANTLA NARAYANA MURTHY

© SRI VISHNU GORANTLA NARAYANA MURTHY, 2016.

Supervisor: Pascal Viala, BMW Group Technology Office USA
Examiner: Torbjorn Thiringer, Chalmers University of Technology, Division of Electric Power Engineering

Master's Thesis 2016
Department of Energy and Environment
Division of Electric Power Engineering
Chalmers University of Technology
SE-412 96 Gothenburg
Telephone +46 31 772 1000

Cover: The grille represent the transition from gasoline to electric cars

Typeset in L^AT_EX
Printed by Chalmers Reproservice
Gothenburg, Sweden 2016

Cell Level Power Electronics for Better Battery Management System
SRI VISHNU GORANTLA NARAYANA MURTHY
Department of Energy and Environment
Chalmers University of Technology

Abstract

In this master thesis, a comparison between two types of battery packs for Electric Vehicles (EVs) is made. Pack 1 is a conventional cells battery pack where all the cells are connected in series. Pack 2 is an autonomous cells battery pack whose cells are equipped with individual micro DC-DC converters. Pack 1 is compared against Pack 2 for energy output (kWh), charging characteristics and ageing. The comparison is performed for two different driving profiles the New European Drive Cycle (NEDC) and a tested and modelled use case.

The DC-DC converter makes Pack 2 the autonomous cells battery pack even though the cells are the same. The DC-DC converter ensures load management on individual cell level. Load balancing leads to several advantages in the energy output, charging characteristics, slower ageing rate and susceptibility to capacity spread of the cells forming the battery pack. The battery pack performances are analysed and compared to show that the performance of Pack 2 is better for both NEDC and use case driving profiles.

A final sensitivity analysis comparing the battery pack ageing is performed for various use cases thus, giving the holistic view of the advantages in the technology used.

Index Terms: Ageing, Battery Management System (BMS), Electric Vehicle (EV), capacity spread, charging characteristics, energy output, lithium ion cell, load management.

Acknowledgements

This thesis work has been performed at BMW Group Technology Office USA, Mountain View, California, United States of America which required a great support from university and industry. I would like to thank my supervisors Dr. Torbjorn Thiringer and Pascal Viala for not only assisting me with technical aspects of the thesis but also providing me an opportunity to learn every day.

I thank Dr. Max von Groll, Robert Richter and Uwe Higgen for providing me an opportunity to write my master thesis with BMW Group and would like to extend it to my colleagues in the Powertrain team and the entire BMW Group Technology Office USA for their co-operation during the progress of my thesis.

To Dr. Simon Lux and Dr. Isaac Lund, a special thanks for taking the time to explain various concepts involved in the cell, assisting me in software modeling and helping me obtain the cell data for implementing the simulation models.

I also extend my thanks to Mehmet Inonu for helping me get the driving data for simulating the use cases.

I will not forget all the interns who helped me maintain between work and fun.

My parents and family in India have been my greatest motivation, support and my backbone during the course of my thesis. I would like to convey my deepest heartfelt thanks to them.

Sri Vishnu Gorantla Narayana Murthy
Mountain View, California, United States of America, 2016

Contents

1	Introduction	1
1.1	Technical Challenge	1
1.2	Previous Work	1
1.2.1	Scope	2
1.3	Purpose	2
2	Theory	3
2.1	Autonomous cells battery pack	3
2.1.1	Cells forming the Battery Pack	4
2.1.2	DC-DC Converter	4
2.1.3	Load	5
2.2	Conventional cells battery pack	5
3	Case Setup	7
3.1	Mathematical Modelling	7
3.1.1	Conventional cells battery pack	17
3.1.2	Autonomous cells battery pack	17
4	Analysis	19
4.1	Energy Output of the Systems	19
4.1.1	State of Charge Comparison	19
4.1.2	Cell Voltage Comparison	22
4.2	Charging Characteristics	24
4.3	Ageing of the Battery Pack	26
4.3.1	Ageing Model	31
4.3.1.1	1C/1C Rate	31
4.3.1.2	C-Rate Determined by NEDC	36
4.4	Impact of Increase in Capacity Spread of the Cells	38
4.4.1	Capacity fade	38
4.4.2	Charging Characteristics	40
4.4.3	Ageing	40
4.4.3.1	1C/1C Rate	40
4.4.3.2	C- Rate Determined by NEDC	41
5	Test Cases	43
5.1	City Driving	43
5.2	Highway Driving	45

6	Use Cases	47
6.1	Percentage Electric Miles	47
6.2	Ageing	51
7	Conclusion	55
8	Future Work	59
A	Appendix	I
A.1	Conventional Cells Battery Pack	I
A.2	Autonomous Cells Battery Pack	III
A.3	Ageing Model	V
	Bibliography	I

1

Introduction

1.1 Technical Challenge

In the present era, the energy usage pattern is shifting from conventional sources such as fossil fuels etc. to renewable energy sources to reduce the carbon footprint. The government is enforcing stringent new regulations [1, 2] to reduce tailpipe emissions and this has affected the automotive industry in a positive way by increasing the demand for Electric Vehicles (EVs) leading to a path of zero emissions in the near future.

A battery pack is the energy storage device used in an EV. In a battery pack, several cells are connected together to form a module and several modules are connected together to meet the load demand from an EV from a battery pack. The cells store electric energy in form of chemical energy. Currently, the battery pack is the most crucial and an expensive component of an EV [3] and requires careful design and optimization to increase the lifetime and operating efficiency of an EV.

To achieve an efficient operation of the battery pack, every battery pack has a Battery Management System (BMS), managing all the cells to yield better performance [4]. All the BMSs now have complex algorithms to ensure cell balancing, prevent cell failures, increase energy output and other functionalities on the pack or a module level but there is no such system whose focus is on load management on the individual cells forming the battery pack.

Cells forming the battery pack are not similar in terms of their capacity and internal resistance [5, 6, 7] irrespective of how accurate the manufacturing environment is. There exist a narrow capacity spread and it is an important issue to be addressed. Due to the existence of this narrow capacity spread, there will always be weaker and stronger cells in the battery pack, thus, affecting its performance.

1.2 Previous Work

A lot of focus has been laid on developing more efficient BMSs and various analysis has been made on parametric variations of cell characteristics forming the battery pack. In few works, simulation models have been developed to propose new systems which deals with parametric variations of the cells [7, 8], but the use of power electronics on a cell level basis is still a topic of research. EV system behaviour analysis needs to be done to see the impact on the energy output, charging time and ageing to assess this new technology.

1.2.1 Scope

Due to the increased complexity involved in simulating the powertrain of an EV, the scope on the analysis of autonomous cells has to be defined to restrict the focus on key aspects. This thesis is framed around analysing the effect of autonomous cells on the powertrain of an EV which comprises of a battery pack, inverter and a motor.

The DC-DC converter in the autonomous cells analysed is modelled through the use of a suitable proportional gain along with a current controlling algorithm and efficiency. The autonomous cells are not optimised for the design of the DC-DC converters on the circuit level. It is assumed that the switching frequency of the DC-DC converter is very high, thus, neglecting the impact of high ripple currents on the cell performance.

In this thesis, the inverter and motor are not optimized and are input from an efficiency map for several different operating conditions in our model.

Compared battery packs are assumed to have a very efficient thermal management system maintaining all cells at the same temperature in both battery packs. This is a valid assumption that can be made to neglect the effect of calendar ageing in this comparison study.

1.3 Purpose

The purpose of this thesis is to compare several key performance factors of a battery pack like energy output, charging characteristics and battery ageing between the conventional cells battery pack and an autonomous cells battery pack. An autonomous cells battery pack is a battery pack whose individual cells are equipped with bi-directional micro DC-DC converters, in which the load on each cell can be controlled independently of the load on the neighbouring cells based on its capacity.

It is proposed that the autonomous cell technology examined in this report helps in several ways like, isolation of a faulty cell and ensuring similar behavior of all the cells in the battery pack as each cell is loaded based on its capacity. All the results are realised by simulations in the Matlab/Simulink environment.

2

Theory

2.1 Autonomous cells battery pack

The new proposed autonomous cells battery pack in terms of an electrical diagram would look like Figure 2.1. It consists of cells forming a battery pack and these cells are connected to a micro DC-DC converter as shown. The output of these DC-DC converters are connected in series to form the DC-link.

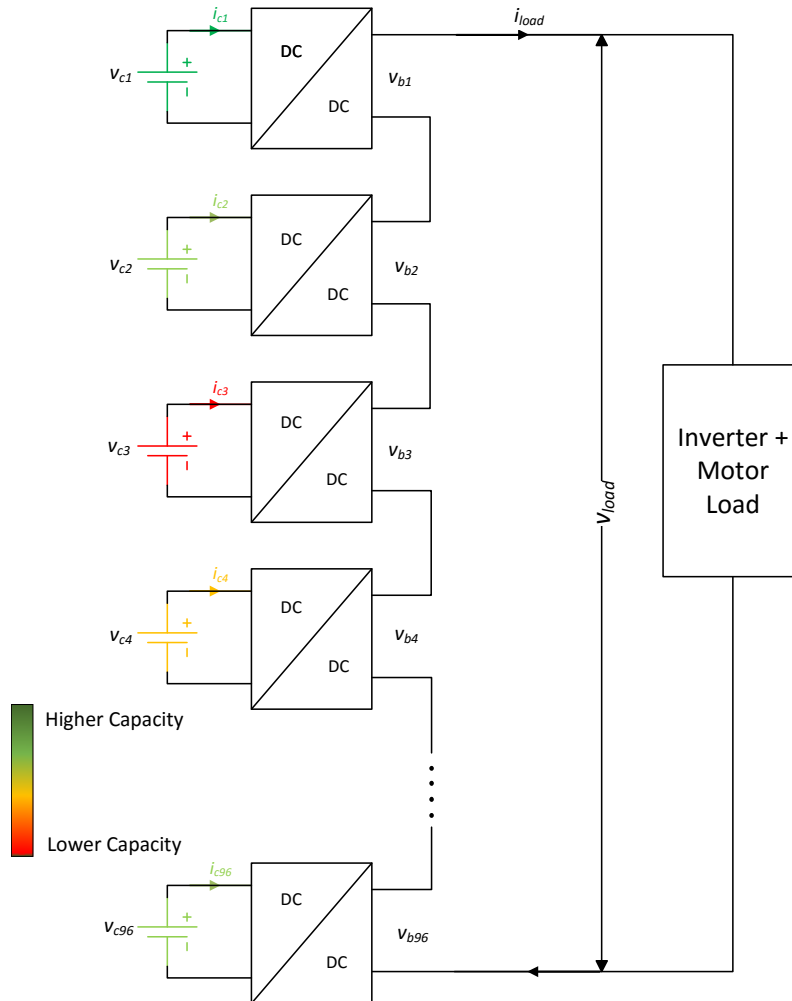


Figure 2.1: Schematic of the proposed autonomous cells battery system

The system comprises of 3 components. They are:

- Cells forming the battery pack
- DC-DC converter
- Load

Each of these components are discussed in more detail in the section below.

2.1.1 Cells forming the Battery Pack

The cells forming the pack are not identical in terms of their capacities [5, 6, 7]. There exists weaker and stronger cells in the pack. This narrow capacity spread of the cells is visualised by different colors as shown in the color map in Figure 2.1. In Figure 2.1 the strongest cell is represented by the brightest shade of green (Cell 1) and the weakest is cell is represented by the brightest shade of red (Cell 3).

The instantaneous cell voltage of the battery pack is represented by $v_{c1}, v_{c2} \dots v_{c96}$ and the instantaneous cell current is represented by $i_{c1}, i_{c2}, \dots, i_{c96}$.

2.1.2 DC-DC Converter

The DC-DC converter serves two major purposes in the system:

- It has to be a bi-directional converter through which the cells are charged and discharged
- To act as an electrical isolation as the cells are not connected directly to each other

The basic flow diagram of the load management algorithm is shown in Figure 2.2.

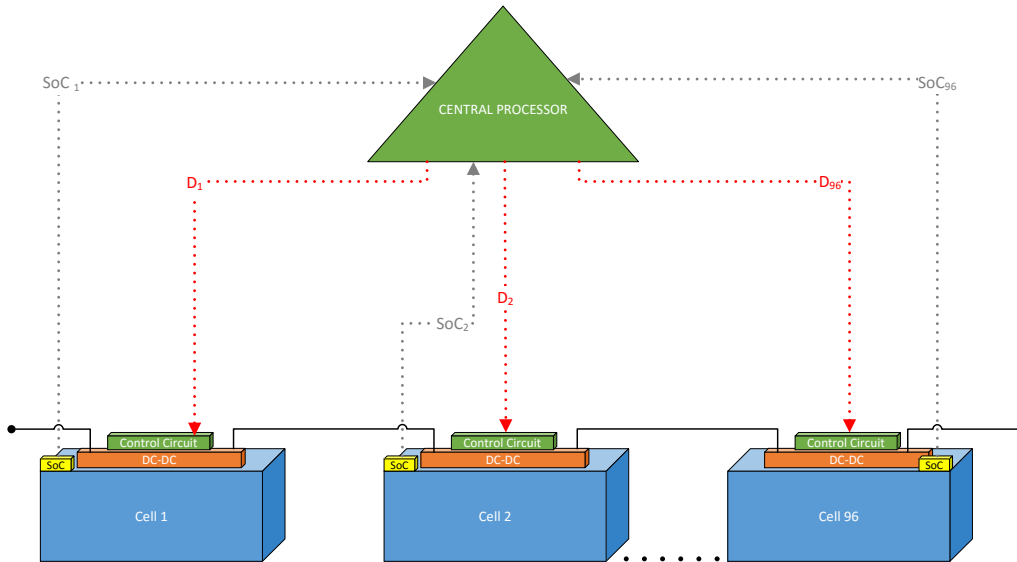


Figure 2.2: Flow of algorithm in the simulated system

The power electronics which controls the autonomous cells works through utilizing a State of Charge (SoC) estimator to measure the initial SoC of the cells [9, 10]. A central microprocessor receives this initial SoC data of all the cells and

classifies the cells. Assuming all the cells are balanced before discharge, the strongest cell is the one with the highest initial SoC and the weakest cell is the one with the lowest initial SoC when the pack is fully charged.

Depending on this data, the central processor computes the duty cycle that is necessary for each individual cell based on its capacity.

The control circuit of the DC-DC converter gets this information and thus, there exists different duty cycles $D_{1...96}$ for each cell which determines the individual cell currents ($i_{c1}, i_{c2}, \dots, i_{c96}$) and bus voltages ($v_{b1}, v_{b2} \dots v_{b96}$) of the system. In this way, the load management operates and the DC-DC converter manages the load on each cell autonomously. The strongest cell carries the highest current and the weakest cell carries the least current so that the SoC of all the cells converge at a particular time.

2.1.3 Load

The load on the battery pack consists of an inverter and a motor. The vehicle is subjected to a drive cycle and the equivalent power in kilo watt (kW) is calculated. This will be the constant power load on the battery given by

$$p_{load} = v_{load}i_{load} \quad (2.1)$$

where,

$$v_{load} = v_{b1} + v_{b2} + v_{b3} + \dots + v_{b96} \quad (2.2)$$

v_{load} is the sum of bus voltages.

$$i_{load} = i_{bus} \quad (2.3)$$

i_{load} is determined by the driving cycle of an EV.

2.2 Conventional cells battery pack

The conventional cells battery pack is the same system as the autonomous cells battery pack but without the DC-DC converter. There exists no load management on individual cell basis unlike the former system. The electric circuit of the conventional system is shown in Figure 2.3.

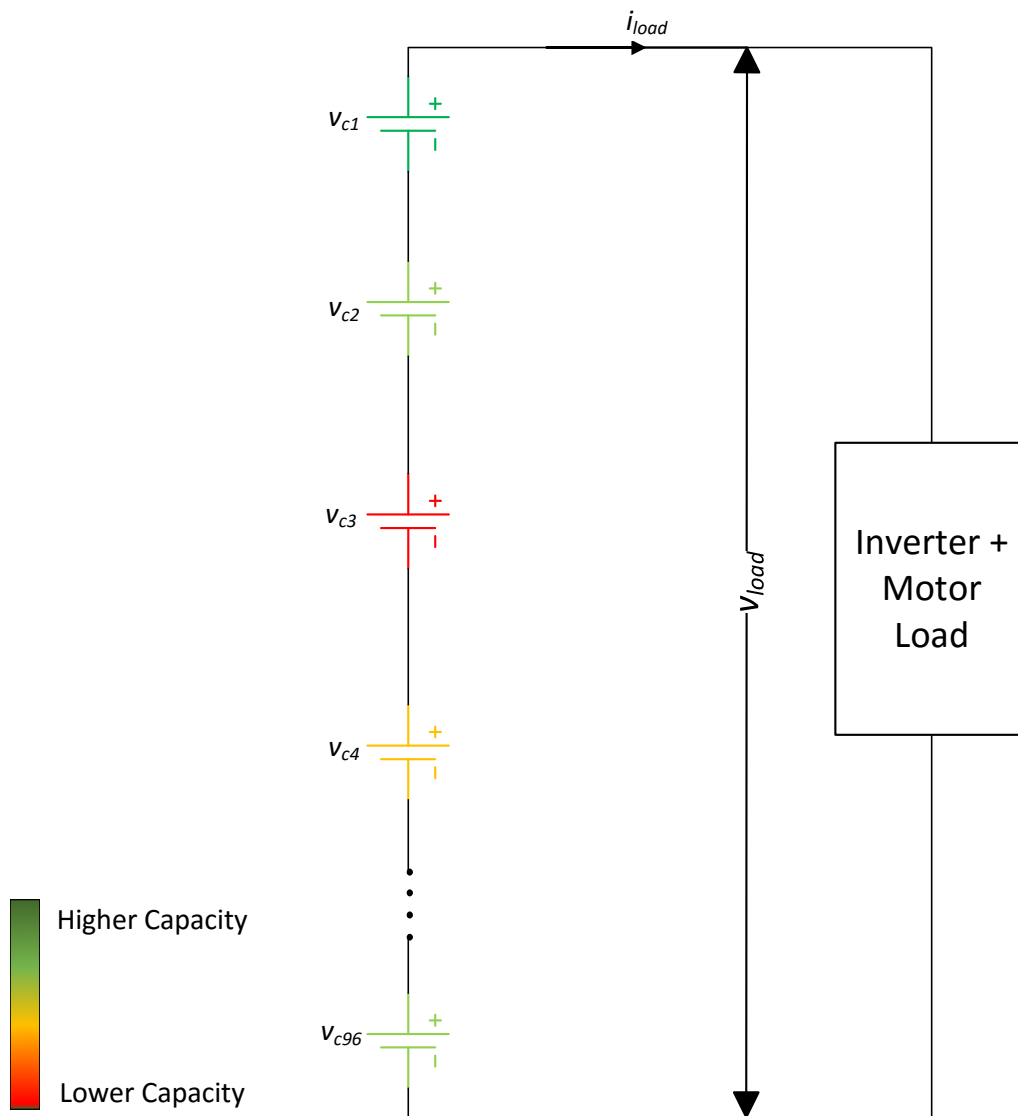


Figure 2.3: Schematic of the conventional cells battery system

Modelling and design of various components are the same for both the systems. In this system,

$$v_{load} = v_{c1} + v_{c2} + v_{c3} + \dots + v_{c96} \quad (2.4)$$

and,

$$p_{load} = v_{load}i_{load} \quad (2.5)$$

where i_{load} is the cell current which is same as the load current. Thus, all the cells, irrespective of its capacity, carry the same magnitude of current.

3

Case Setup

In this thesis, a detailed analysis between two types of BMS is conducted in the Matlab/Simulink environment. The simulation set-up for both these cases are explained in the sections below.

A battery pack may consist of 8 modules. Each module consists of 12 cells connected in series. Thus, the battery pack consists of 96 individual cells. Here, the cell technology is Li-ion and all cells are connected in series to meet the load demand.

3.1 Mathematical Modelling

Figure 3.1 shows the different components of the system that are modelled in the simulation environment.

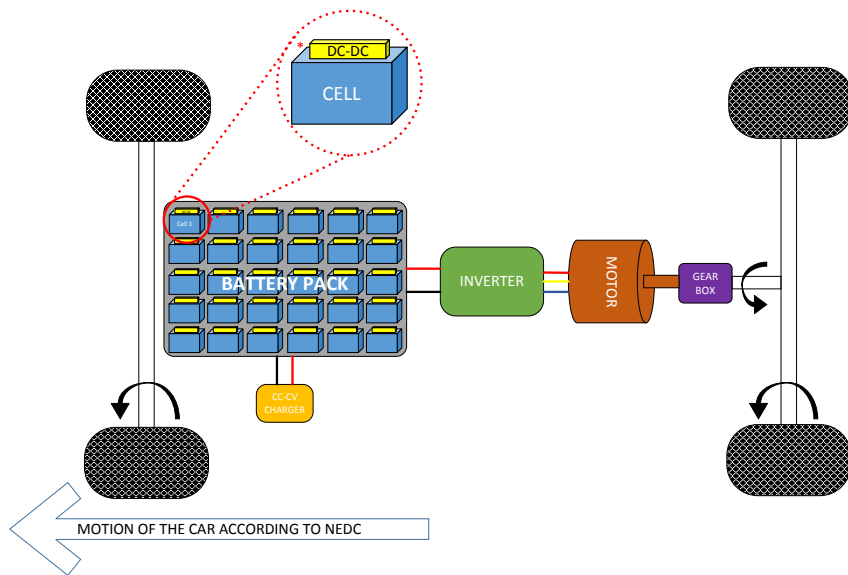


Figure 3.1: Overview of the modelled system

Various loads acting on the battery pack is shown in Figure 3.1. In Figure 3.1 the components to the right hand side of the battery pack represents the

3. Case Setup

various loads connected to it. The battery pack is designed to supply the forces experienced by the vehicle while driving, losses experienced by the inefficiencies in motor/inverter and inefficiencies in battery. To have a complete system, a Constant Current - Constant Voltage (CC-CV) charger is also modelled and explained in the upcoming sections.

Battery: In this simulation, cells are modelled as a Coulomb counter which is a pure current integrator. Before the discharge event, all the cells are assumed to be balanced and charged to the upper cut-off voltage and the SoC corresponding to this voltage is the initial SoC. This Coulomb counter can be mathematically represented by

$$SoC = \int I_{cell} dt + c \quad (3.1)$$

Here, I_{Cell} is the cell current and c is a constant that represents the model's initial condition. In this case, it is initial SoC, then, (3.1) can be written as

$$SoC = \int I_{Cell} dt + InitialSoC \quad (3.2)$$

The Open Circuit Voltage (OCV) is obtained by using the look-up table of OCV vs SoC characteristic which is shown in Figure 3.2. The graph contains 96 cells forming the battery pack. Each individual cell has its own OCV vs SoC characteristic which is normally distributed.

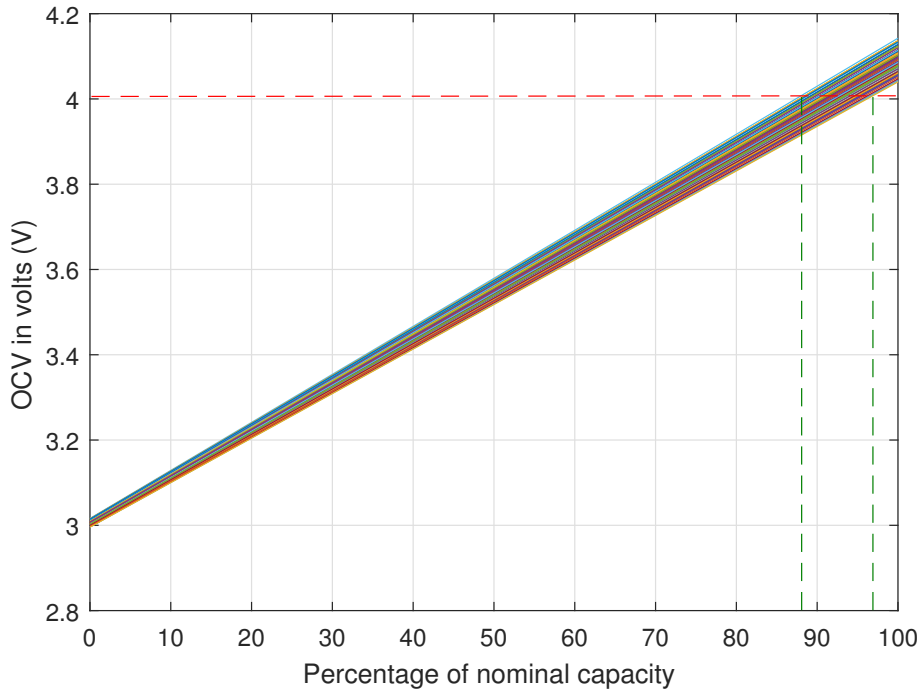


Figure 3.2: OCV plot to obtain the initial Ah of the cells

As seen in Figure 3.2, there is a slight deviation in OCV vs SoC , which is caused by the Gaussian spread in the capacity from the targeted manufactured

capacity of the cells forming the battery pack. In simulations, it is assumed that all the cells are balanced [11] and have an OCV of 4.035V and the SoC corresponding to this voltage are considered as the initial condition to the battery model designed in the Matlab/Simulink environment. This Gaussian distributed initial SoC has a mean (μ) of 94.99% and a standard deviation (σ) of 2.18%.

With the knowledge of OCV , the cell voltage is calculated by using Kirchhoff's voltage law (KVL) where,

$$V_{cell} = V_{OCV} + I_{cell}R_i(SoC) \quad (3.3)$$

where, $R_i(SoC)$ is the DC-Internal Resistance (DC-IR) dependent on the SoC of the cell. All the 96 cells are assumed to have the same values of $R_i(SoC)$.

Load Modelling: The simulation model is adopted to a constant power load which is calculated from the New European Drive Cycle (NEDC) [12] as shown in Figure 3.3. The NEDC comprises of 4 city cycles and 1 highway cycle.

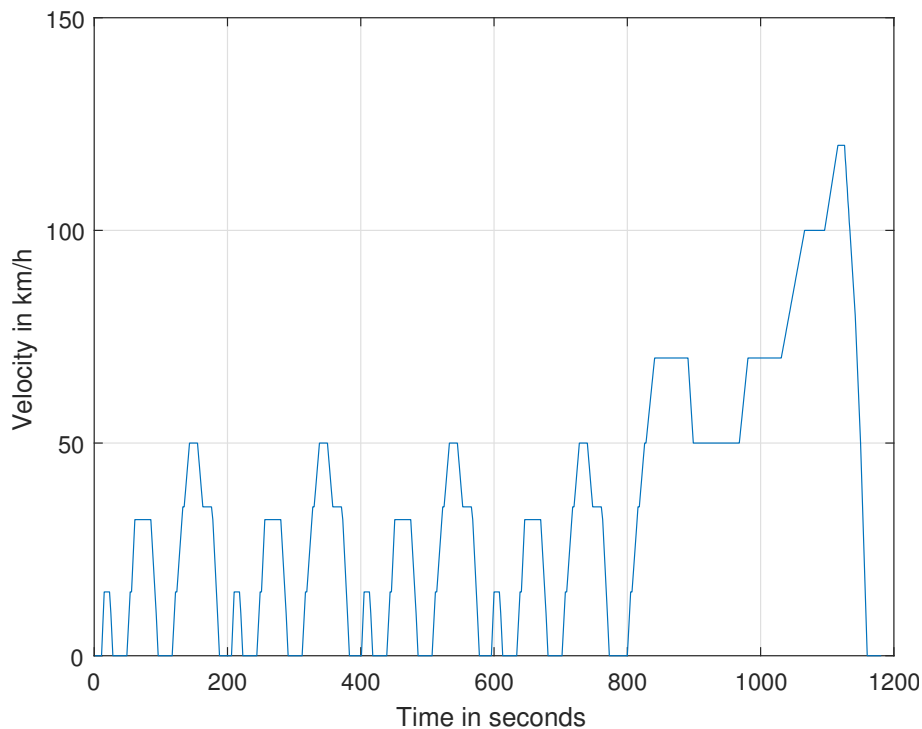


Figure 3.3: New European Drive Cycle - A standard driving profile

The speed from this drive cycle is converted to equivalent electric power by using simple mechanical equations and driving dynamics of the car. For the sake of simplicity, the forces acting on the car are assumed to be air resistance on the car (F_{drag}), rolling friction (F_{rf}) and force due to acceleration (F_{acc}). The power (P) is calculated from the NEDC using a simple unicycle model of a car. The mechanical equations governing this system are

$$P = (F_{drag} + F_{rf} + F_{acc})v \quad (3.4)$$

3. Case Setup

$$F_{drag} = \frac{1}{2}\rho Av^2 C_x \quad (3.5)$$

where, ρ is the air density = $1.225kg/m^3$,
 A is the surface area of the car = $2.38m^2$,
 v is the velocity of the car in m/s determined by the drive cycle,
 C_x is the co-efficient of drag = 0.30 ,
furthermore,

$$F_{acc} = ma \quad (3.6)$$

where, m is the mass of the car = $1200kg$
 a is the acceleration of the car in m/s^2

$$F_{rf} = constant \quad (3.7)$$

here, the rolling friction is assumed to be a constant value as it does not vary significantly with the velocity of the car, thus, its impact on the power obtained is fairly constant.

The power obtained (kW) from one NEDC is shown in Figure 3.4. Here it is seen that there exists both positive and negative values of power which signifies acceleration and recuperation events. The plot below shows the values of power without any efficiency calculations performed. The efficiency calculation is implemented in the next section.

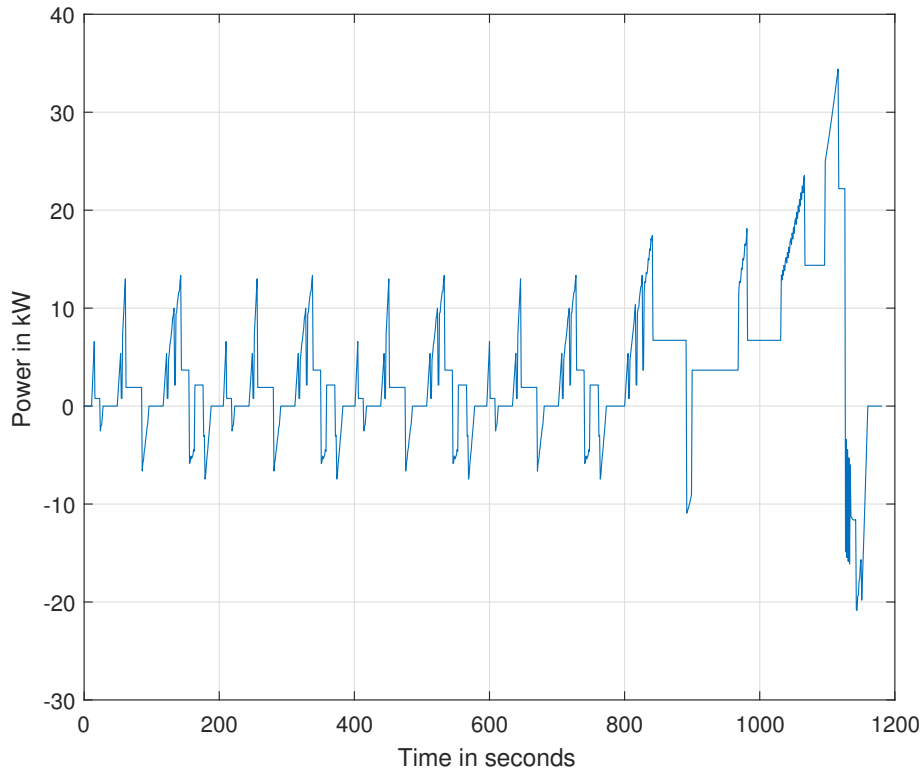


Figure 3.4: Power demand on the pack from 1 NEDC

The peak power experienced by the cell is around 35 kW . This is usually too low to be used as a dimensioning power for a car and it depends on the drive cycle under consideration. The considered drive cycle is not representative of all types of driving.

Efficiency of Motor, Inverter and Gear-Box: A look-up table for the motor efficiency is created by using the torque-speed and efficiency characteristics. The positive power calculated according to (3.4) is divided by the efficiency to get the actual power demand on the battery pack and the negative power is multiplied by the efficiency to simulate the losses in the recuperation system.

The inverter loss and the gear-box model is not dealt with as it falls out of the scope of this thesis. The inverter efficiency is assumed to be 97% and the reduction gear box efficiency is assumed to be 90%

The new plot comparing the power demand from NEDC is shown in Figure 3.5. The battery pack must be able to supply the losses as well, this means that the power demand on the battery pack is more that the power demand from the NDEC itself. This is shown in the red curve below.

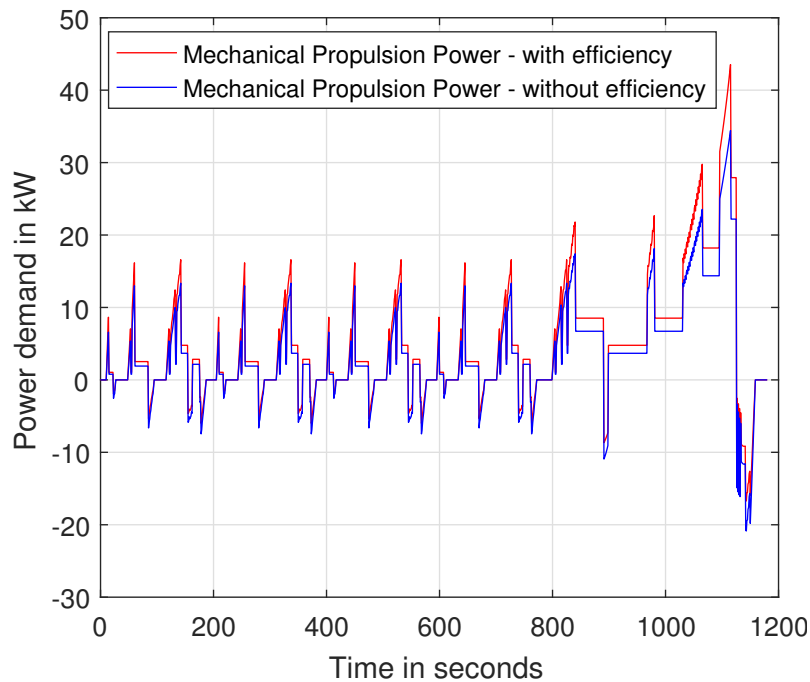


Figure 3.5: Power demand comparison with and without efficiency considerations of the system over 1 NEDC

Table 3.1 consolidates all the results and indicates the energy requirement on the battery pack for 1 NEDC. These results include all the calculated efficiencies in the system.

Table 3.1: Simulated System

Characteristic	Value
Time per Cycle (<i>s</i>)	1180
Distance Travelled (<i>km</i>)	11.0121
Total Energy Required (<i>kWh</i>)	1.5042
Energy per <i>km</i> (<i>kWh</i>)	0.1366

DC-DC Converter: The basic functionality of the BMS was explained earlier. Based on this, the DC-DC converter is modelled in Matlab/Simulink. The DC-DC converter has a proportional controller for each individual cell in the battery pack. For the design simplicity, we assume that the DC-DC converter is ideal (i.e.),

$$V_{cell}I_{cell} = V_{bus}I_{bus} = V_{bus}I_{load} \quad (3.8)$$

Since the cell current I_{cell} is higher for a stronger cell and lower for a weaker cell, the load management on individual cell during discharge take place based on

$$I_{cell} = \frac{SoC(initial)}{SoC(max)} I_{load} D \quad (3.9)$$

Here, the initial SoC is the SoC corresponding to the OCV of 4.035V where all the cells are assumed to be balanced and D is the duty cycle computed by the central processor and is given by

$$D = \frac{V_{bus}}{V_{cell}} \quad (3.10)$$

A similar situation takes place when the cells are charged. The stronger cell is charged at a higher charging rate than the weaker cell. The charging current is determined by

$$I_{cell-ch} = \frac{1 - SoC(max)}{1 - SoC(initial)} I_{ch} \quad (3.11)$$

Here, the initial SoC is the SoC corresponding to the OCV of 3V assuming the cells are balanced at the end of discharge period.

The loss calculations are made separately for the DC-DC converter with the help of an efficiency map provided by the manufacturer. It is assumed that the performance of all the 96 DC-DC converters follow the same efficiency map irrespective of its duty cycle and performance history. This is shown in Figure 3.6.

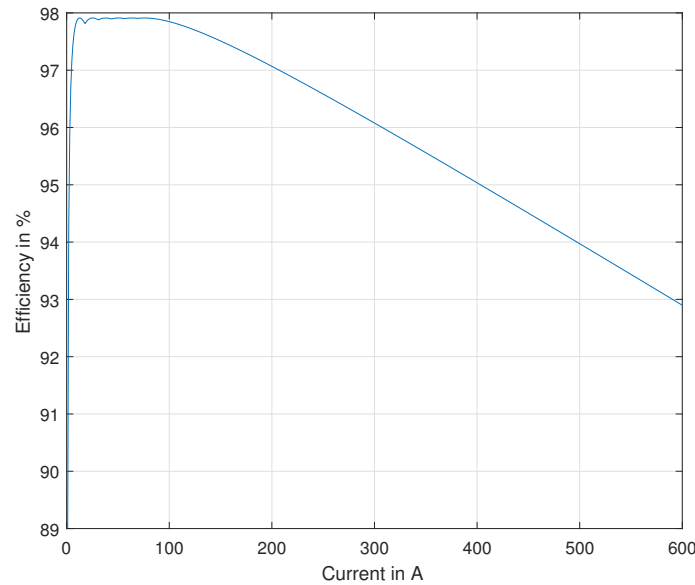


Figure 3.6: Current vs Efficiency of the DC-DC converter

In a conventional cells battery pack, there are no DC-DC converters on top of each cell, but in the autonomous cells battery pack, the battery must be able to provide energy for the losses incurred in DC-DC converter as well. Thus, the power demand on the conventional cells battery pack is slightly lesser than the power demand on the autonomous cells battery pack.

Constant Current - Constant Voltage Charging: The CC part of the charger is just a constant value of 1C (explained in the next section), the controller monitors the cell voltage continuously and when the weakest cell reaches 4V, the transition to CV takes place on the pack level. The charger in CV mode is modelled as a proportional controller with a gain being the reciprocal of internal resistance of the cell. The reference voltage is set to 4.1V, based on difference between the instantaneous cell voltage, reference voltage and DC-Internal Resistance (DC-IR), the controller outputs a value of the charge current necessary to keep the cell voltage constant.

In case of using autonomous cells, the charging takes place purely on the capacity of the cells. In this case, the transition to CV mode occurs on an individual cell basis. This is discussed in detail in Chapter 4.

Ageing Model: The battery pack is a crucial component of an EV. It is important to develop new BMSs whose focus should be to prolong the battery pack life. A prolonged battery pack life not only encourages the consumers to buy an EV, but also improves the end-to-end life cycle of the battery pack. Thus, it is a big asset to have a slower ageing rate.

Cell ageing depends on several factors like temperature, loss of anode material, loss of lithium ions, Solid Electrolyte Interface (SEI) layer formation and many other factors [13, 14, 15].

Two mechanisms play a significant role in loss of cell capacity are: cycle ageing and calender ageing. Cycle ageing is the number of charge-discharge cycles a cell can be subjected to before reaching its End of Life (EOL) and it depends on

the cell current and SoC. Calender ageing is the time in years that a cell can be stored before reaching its EOL. Calender ageing occurs due to self discharge of the cell and it depends on cell temperature.

The two battery packs under comparison are assumed to have a very efficient thermal management system, thus, all cells are maintained at the same temperature, thereby, neglecting the effect of calender ageing. Only cycle ageing (hereby ageing) comparison is carried out in this thesis.

The initial step is to get an idea of the amount of time a cell under consideration spends in various current regions. This can be done by plotting a histogram of current over 1 complete discharge-charge cycle (hereby cycle). From this result, it is important to estimate the ageing benefit quantitatively. This is done by assigning an empirical damage factor for both current and SoC for different regions of operation obtained by discussions with battery experts.

Thus, the capacity loss in the ageing model built in this thesis is given by

$$C_{Loss} = f(I_{Cell}, SoC) \quad (3.12)$$

The capacity loss (C_{Loss}) due to ageing can be computed by calculating the total damage factor (α_T) on the cell due to cycling.

As C_{Loss} depends on current and SoC of the cell, the total damage factor (α_T) of the system also depends on current and SoC of the cell and is given by,

$$\alpha_T = \sum_{n=1}^{N_{max}} \alpha_i(n) + \sum_{n=1}^{N_{max}} \alpha_{soc}(n) \quad (3.13)$$

where, α_i is the damage factor in Ah/h due to current flowing in the cell, α_{soc} is the damage factor in Ah/h due to the SoC of the cell, N_{max} is the maximum number of cycles before the cell reaches its EOL

The damage factor for the current (α_i) is assigned based on the C-rate as shown in Figure 3.7. The negative C-rates signify charging event and the positive C-rates signify the discharging event of the battery pack.

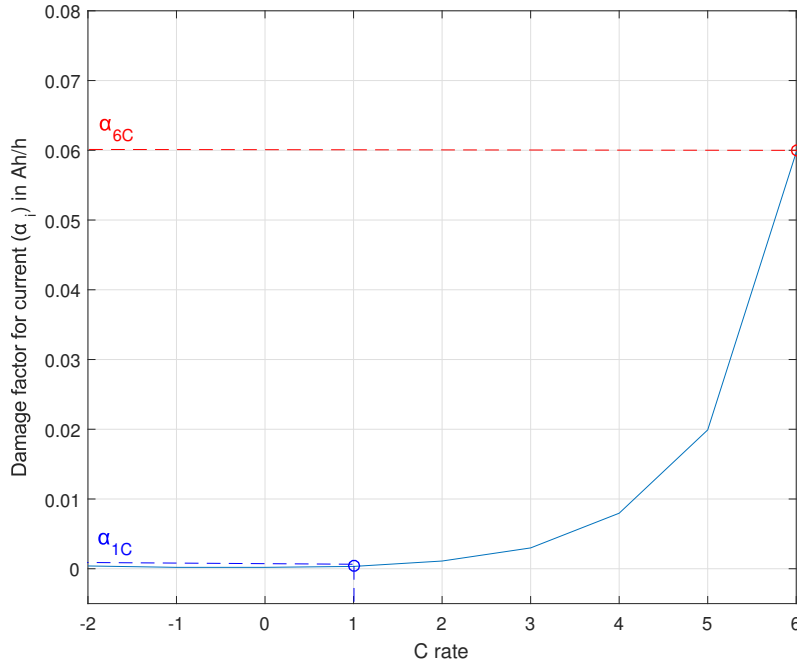


Figure 3.7: Damage factor vs C-rate

The higher the C-rate, the higher the damage on the cell, thus, a higher damage factor applies, similarly, the lower the C-rate, the lower the damage on the cell, thus, a lower damage factor applies. The damage factor is usually exponential in nature, but for the sake of simulation purpose, several linear functions with different slopes are considered.

The total damage factor (α_T) is calculated below,

1. To calculate the damage factor for current (α_i), a few assumptions must be made. The EOL criteria is that cell loses 10 % of its capacity (ΔAh) when it is subjected to 3000 cycles at 1C. Ideally, a cell takes 1 hour to completely discharge when discharged at 1C and it takes 1 hour to completely charge when charged at 1C.

Thus, the time in hours the cell spends during 1 cycle

$$h = 2 \times 3000 \quad (3.14)$$

A general expression for the damage factor for the cell current is

$$\alpha_i = \frac{\Delta Ah}{h} \quad (3.15)$$

The damage factor of the cell for a 1C cycle α_{1C} is given by,

$$\alpha_{1C} = \frac{10 \times Ah_{rated}}{100 \times (2 \times 3000)} = \frac{10 \times 20}{100 \times (2 \times 3000)} = 3.333 \times 10^{-4} Ah/h \quad (3.16)$$

This means that the cell loses $3.333 \times 10^{-4} Ah$ with every charge and discharge cycle due to the current for 1C discharge rate.

3. Case Setup

A similar calculation is performed for 6C where we assume ΔAh is achieved after 100 cycles,

$$\alpha_{6C} = \frac{10 \times Ah_{rated}}{100 \times (2 \times 100)} = \frac{10 \times 20}{100 \times ((2/6) \times 100)} = 0.06Ah/h \quad (3.17)$$

This means that the cell loses $0.06Ah$ with every charge and discharge cycle due to the current for a 6C discharge rate.

The two points α_{1C} and α_{6C} are fixed and act as a boundary condition as shown in the graph. The damage factors at other C-rates viz. ($\alpha_{2C}, \alpha_{3C}, \dots, \alpha_{5C}$) can be adjusted as necessary to study the ageing behaviour of the system.

While cycling the cell, it must be considered that the capacity of the cell is constantly reducing with every cycle. This means that, as the cell ages, the actual capacity available reduces, thus, the new C-rate is to be computed based on the new capacity. Doing this impacts the damage factor (α_i) and gives us a more realistic value.

2. The impact of SoC is also considered to calculate ageing. A similar approach is used wherein the SoC is divided into different regimes. This is shown in Figure 3.8.

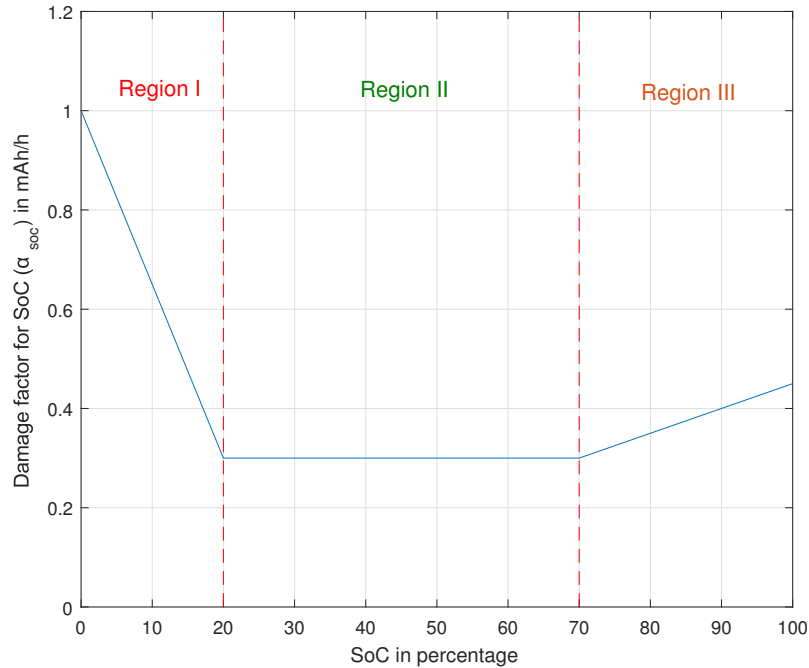


Figure 3.8: Damage factor vs SoC

The damage factor for SoC (α_{soc}) is divided into three regions which are color coded. Green represents safe operation region with a lower damage factor and the transition to red represents unsafe region with a higher damage factor. Depending on the cell's SoC in these regions, a suitable damage factor (α_{soc})

is chosen. In the green region, the cell attains its chemical equilibrium, thus, it has a lower damage factor as opposed to the remaining two regions.

While cycling the SoC of the cell, it must be taken care that the capacity of the cell is constantly reducing with every cycle. This means that, as the cell ages, the actual capacity available is reduced, thus, the new SoC is to be computed based on the new capacity. Doing this impacts the damage factor (α_{soc}) and gives us a more realistic value.

The damage factor for current (α_i) and the damage factor for SoC (α_{soc}) is summed according to (3.13) and is subtracted from the actual capacity of the cell to get the new capacity after considering the effect of ageing in terms of damage factor (α_T).

New capacity C_{New} in Ah is given by,

$$C_{New} = C_{Rated} - C_{Loss} \quad (3.18)$$

where, C_{Loss} in Ah is given by,

$$C_{Loss} = \alpha_T h \quad (3.19)$$

Finally, to analyse the ageing behavior, the weakest cell in a conventional cells battery pack and the weakest cell in autonomous cells battery pack is compared. Since, the strongest cell in autonomous cells battery pack carries a higher magnitude of current and discharges deeply compared to the weakest cell, it is important to make sure that the ageing of the strongest cell is proportional to its capacity. Thus, the strongest cell in an autonomous cells battery pack is also considered in the ageing comparison study.

3.1.1 Conventional cells battery pack

In a conventional cells battery pack, the mathematical models derived are connected in series and are simulated in the Matlab/Simulink environment.

3.1.2 Autonomous cells battery pack

In this approach, the mathematical models along with the DC-DC converter is simulated and compared against the conventional cells battery pack.

Both the systems are subjected to the same initial conditions and the same *OCV vs SoC* characteristic. Various attributes of the battery pack are plotted to compare and analyse the behavior of the system. The detailed analysis will be made in the upcoming chapters.

4

Analysis

4.1 Energy Output of the Systems

The conventional cells battery pack and the autonomous cells battery pack is compared in terms of energy output and range when it is subjected to several NEDCs till the lower cut-off voltage of the battery pack is reached.

Both the battery packs have same conditions of inverter and motor efficiency, the same efficiency in recuperation and also same battery losses. The only and major difference in the autonomous cells battery pack is that the efficiency of all the 96 DC-DC converters are also considered for the load demand.

4.1.1 State of Charge Comparison

The strongest cell is the one with the highest initial SoC and the weakest cell is the one with the lowest. The considered capacity spread has a mean $\mu = 95\%$ and standard deviation $\sigma = 2.18\%$.

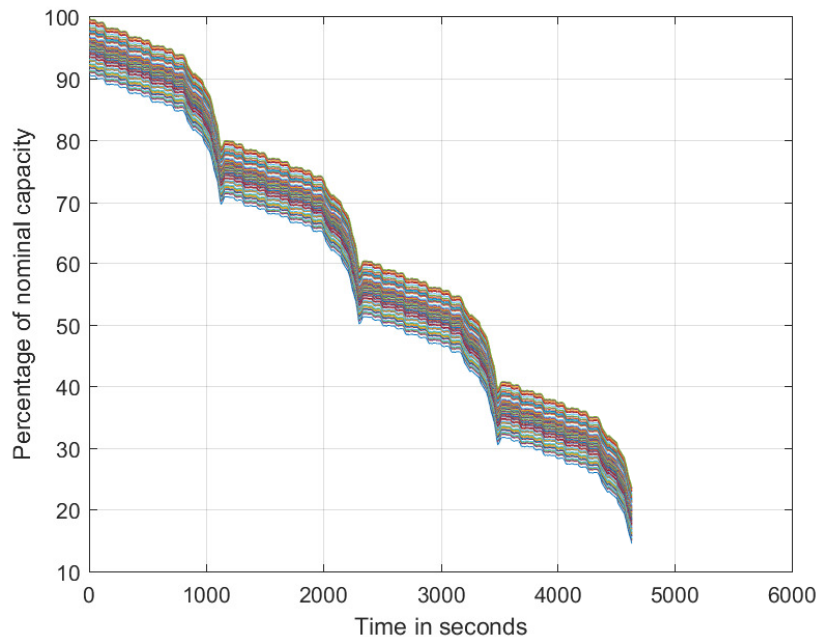


Figure 4.1: Percentage of nominal capacity of 96 cells in conventional cells battery pack

In the conventional cells battery pack, as shown in Figure 4.1 there is no SoC matching between the cells, thus, the stronger cell and the weaker cell are stressed at the same level. Due to this, the weaker cell hits the lower voltage cut-off limit first and the discharge is stopped for the whole pack. Here, the battery pack discharge performance is limited by the weakest cell because there is no cell level load management and thus, all the cells carry the same current as shown in Figure 4.2.

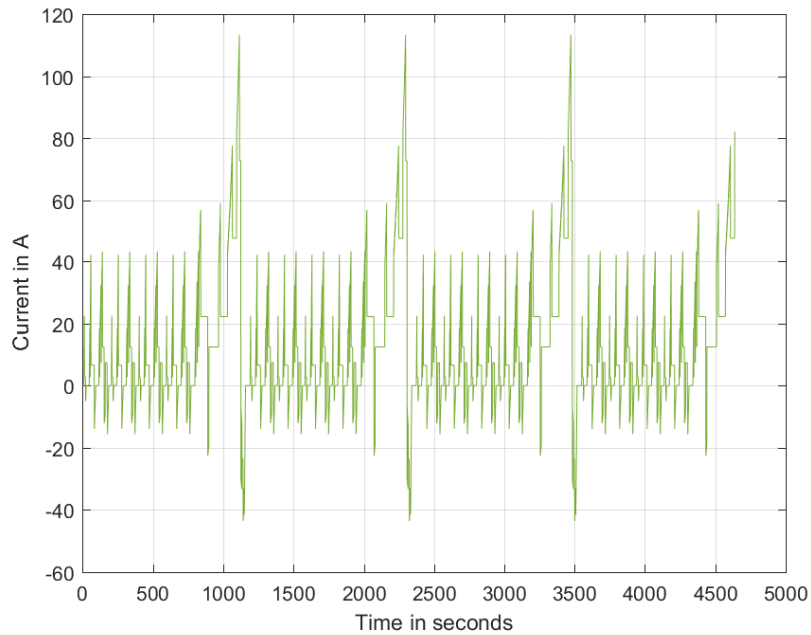


Figure 4.2: Current of 96 cells in the conventional cells battery pack

In contrast to this, the SoCs of all the cells in the autonomous cells battery pack are matched due to the DC-DC converter. As a result of this SoC matching, the stronger cells are stressed more than the weaker cells until the SoC of the cells are matched. This ensures that all the cells reach the lower voltage cut-off limit at the same time and the battery pack discharge dependency on the weakest cell is eliminated, thus, the discharge lasts longer yielding to more energy output from the pack. This is clearly seen in Figure 4.3 compared to Figure 4.1.

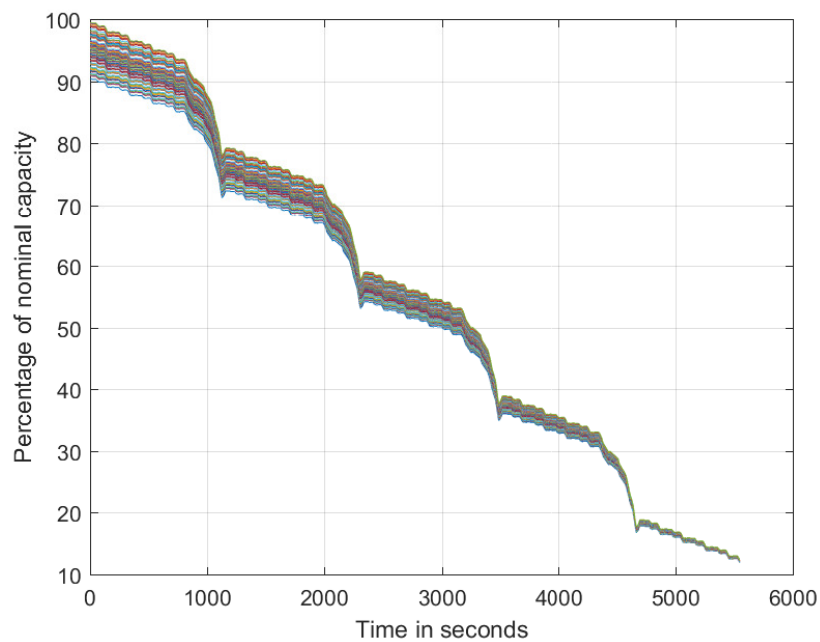


Figure 4.3: Percentage of nominal capacity of 96 cells in autonomous cells battery pack

This behavior of SoC is observed because, the DC-DC converter ensures that there is load management on individual cell and thus, the weaker cell carries a lesser current and the stronger cell carries a higher current as shown in Figure 4.4.

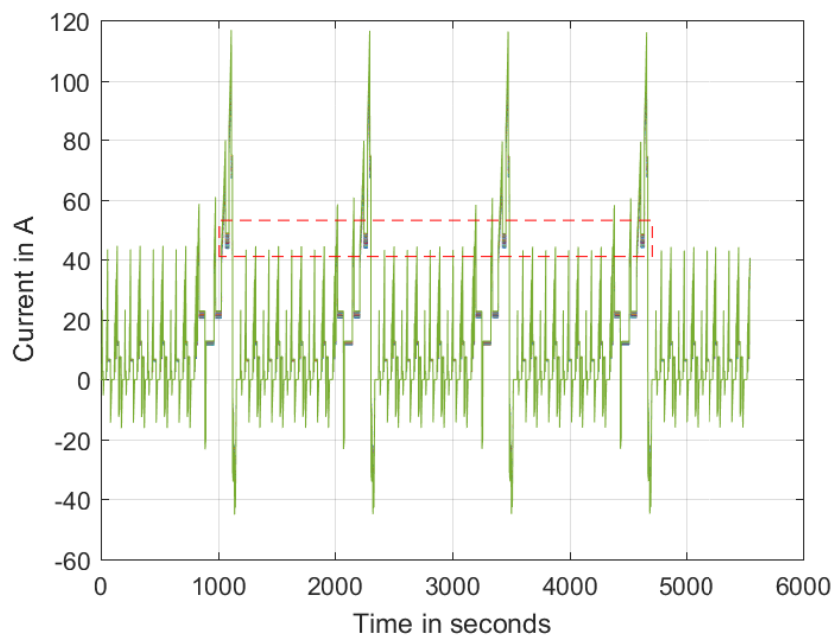


Figure 4.4: Current of 96 cells in the autonomous cells battery pack

By magnifying the dashed rectangular window in Figure 4.4, the spread

of the current can be understood correctly. This is shown in 4.5. The stronger cell carries a higher current in the first cycle, the control system monitors the SoC and as the SoC reduces, the current drawn by the stronger cell also reduces over a discharge cycle. If the discharge cycle is long enough, the cells are stressed such that, eventually at a particular time, all the cells have the same SoC and thus, experience the same current. This occurs because the individual DC-DC converters makes sure that the stronger cells are stressed more than the weaker cells till all the cells reach the same capacity.

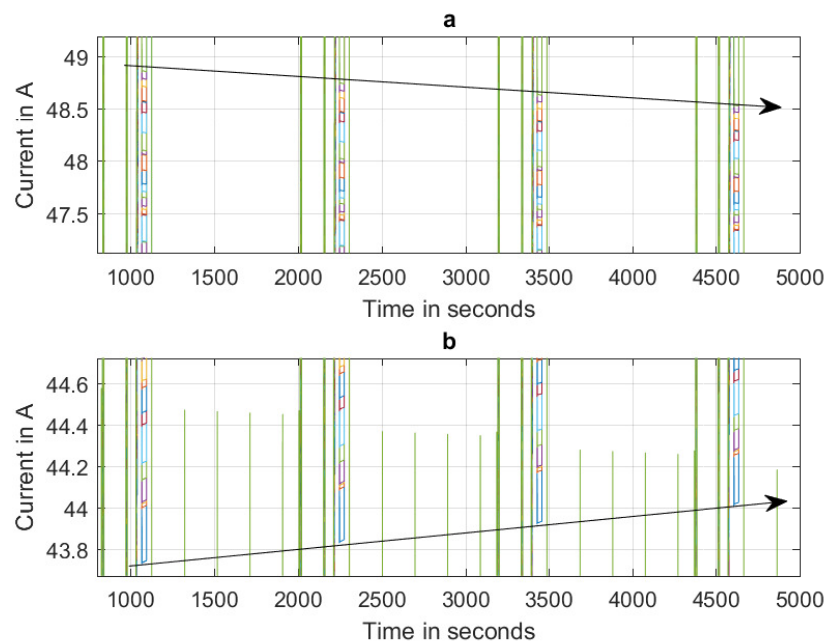


Figure 4.5: Converging trend in the cell currents - Magnified at the dashed red window in Figure 4.4

Plot (a) represent the decreasing trend in the strongest cell current and plot (b) represent the increasing trend of the weakest cell current. Thus, Figure 4.5 represent the converging trend of the cell current in case of using the autonomous cell battery pack.

4.1.2 Cell Voltage Comparison

The observed differences in the SoC results from the current within the cells. The current carried by individual cells are managed by the DC-DC converter based on the cell's capacity. Due to the different behavior of the SoC of the cells in the battery pack, there is also a difference in cell voltage. This is plotted in Figure 4.6. The red colored plot represents all the 96 cells forming the autonomous cells battery pack where as, the green colored plot represent all the 96 cells forming the conventional cells battery pack.

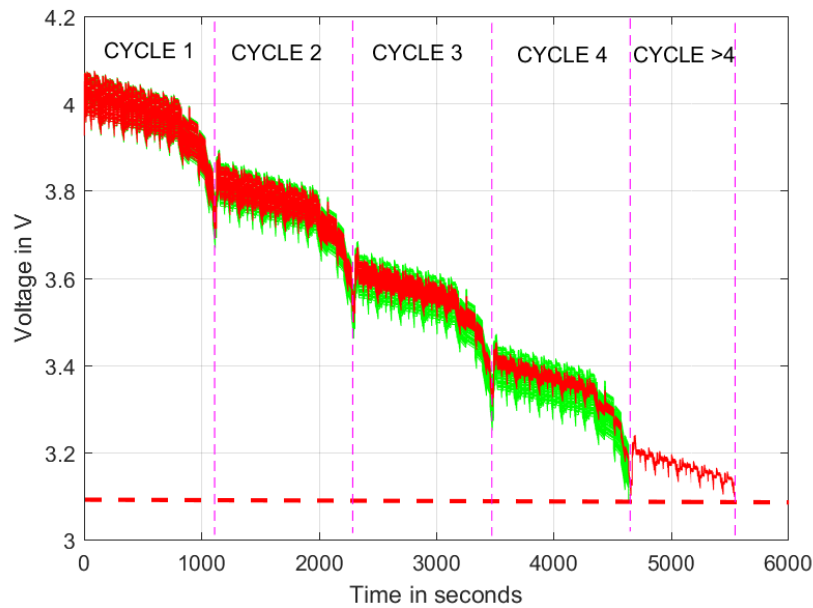


Figure 4.6: Cell Voltage of 96 cells - Green: Conventional cells battery pack; Red: Autonomous cells battery pack

The cell voltage characteristics of both the battery packs overlap. It is seen that the cells forming the autonomous cells battery pack hit the lower voltage cut-off limit (shown in the dashed red line) later than that of the conventional cells battery pack. This translates to a time of 909 seconds per discharge cycle. Thus, the energy of the autonomous cells battery pack yields a higher energy compared to the conventional cells battery pack.

Table 4.1 compares the energy output of the two considered battery packs.

Table 4.1: Simulated results for $\mu = 95\%$ and $\sigma = 2.18\%$

	Autonomous Pack	Conventional Pack
Range (<i>km</i>)	48.29	42.47
Energy Output (<i>kWh</i>)	6.65	5.8
Cut-off Time (<i>s</i>)	5549	4640
ΔV (<i>mV</i>)	1.00	101

Here, ΔV is the difference in voltage between strongest cell and the weakest cell at the end of discharge and is given by

$$\Delta V = V_{strongest} - V_{weakest} \quad (4.1)$$

It is obvious that the difference in the cell voltage is much more significant in case of using a conventional cells battery pack. This implies that, the cells in the conventional cells battery pack are not balanced well in this case and there exists a need for passive balancing circuits unlike the cells in the autonomous cells battery pack where the cells have similar voltage levels.

4.2 Charging Characteristics

The cells are charged in a CC-CV (Constant Current-Constant Voltage) algorithm. The simulation is performed for 6000s. This is done because the simulation dynamics are too slow and it takes a long time for the SoC to reach the set point value in conventional cells battery pack charging. To simulate charging, the same battery model is used but the initial condition to the model here is the SoC corresponding to 3.1V (assuming all cells are balanced after discharge) and the load is a CC-CV algorithm block, supplying current to the battery.

In a conventional cells battery pack, in CC mode, all the cells irrespective of their capacities, carry the same current, leading to a quicker charging of the weaker cells. The moment when the weakest cell reaches 4.0V, the entire system is switched to CV mode. Here the current tapers down as the cell voltage is maintained constant. The stronger cells see the CV mode even before reaching the 4.0V limit. This increases the total charging time in the CV mode. In this case, the transition to CV mode depends on the weakest cell in the pack and this characteristic is shown in Figure 4.7

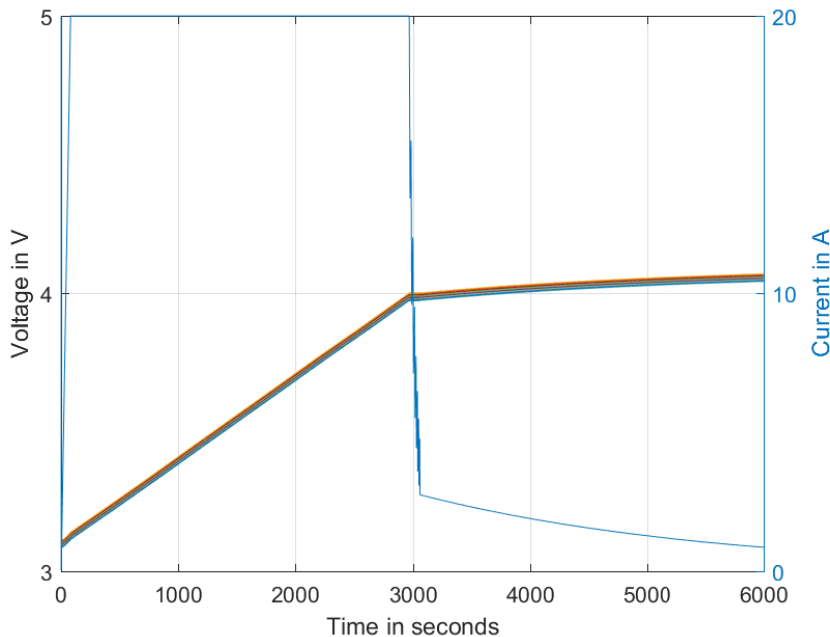


Figure 4.7: CC-CV charging on the conventional cells battery pack

Here, it can be observed that the current flowing through all the cells in the conventional cells battery pack is the same, moreover, at the end of 6000s, the cell voltages are not balanced, thus, there exists a necessity to use passive balancing circuits to achieve same cell voltages on all the cells in the battery pack.

The SoC during the charging serves as a better visualisation to the transition from CC to CV mode.

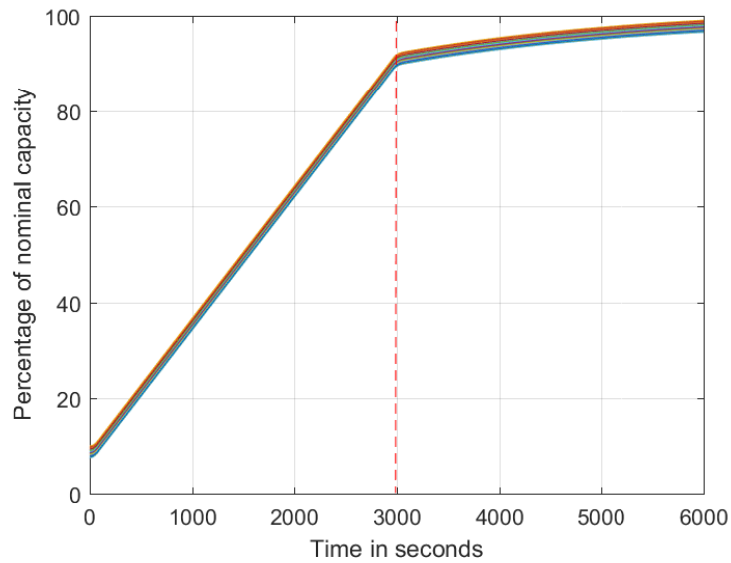


Figure 4.8: Percentage of nominal capacity of all the 96 cells in conventional cells battery pack

As shown by the red dotted line in Figure 4.8, the weakest cell hits 4.0V and all the cells are transitioned to CV mode.

In the autonomous cells battery pack, cells are charged based on their individual capacity. All the cells are individually monitored and the current flowing through the cells are independently maintained. This leads to a more uniform voltage profile of all the cells in the pack, thereby, eliminating the need for passive balancing circuits.

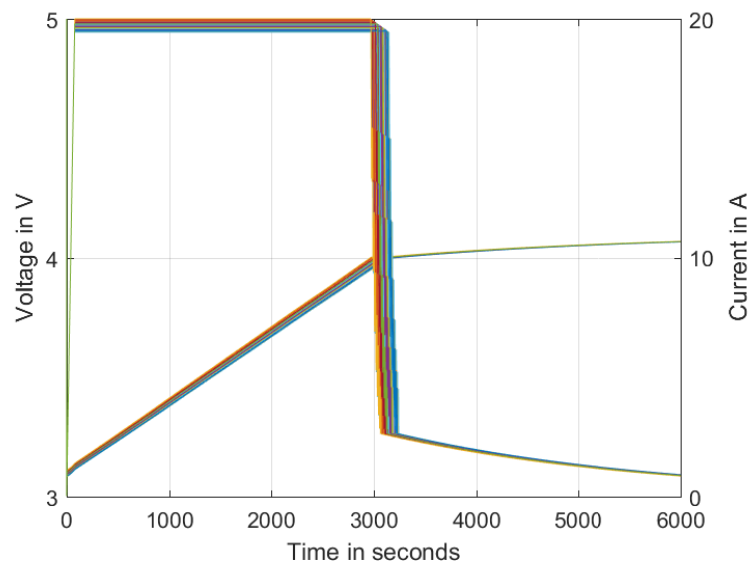


Figure 4.9: CC-CV charging on the autonomous cells battery pack

As shown in Figure 4.9, there are 96 different charging currents monitored by the individual DC-DC converter present on each cell. The strongest cell is charged

at 1C and the weakest cell is charged at a current less than 1C depending on its capacity according to equation 3.11. This allows each cell to charge independently and thus, the CC charging can be done when the cells in the pack reach 4.0V. The plot shown in Figure 4.10 gives a better illustration of the situation.

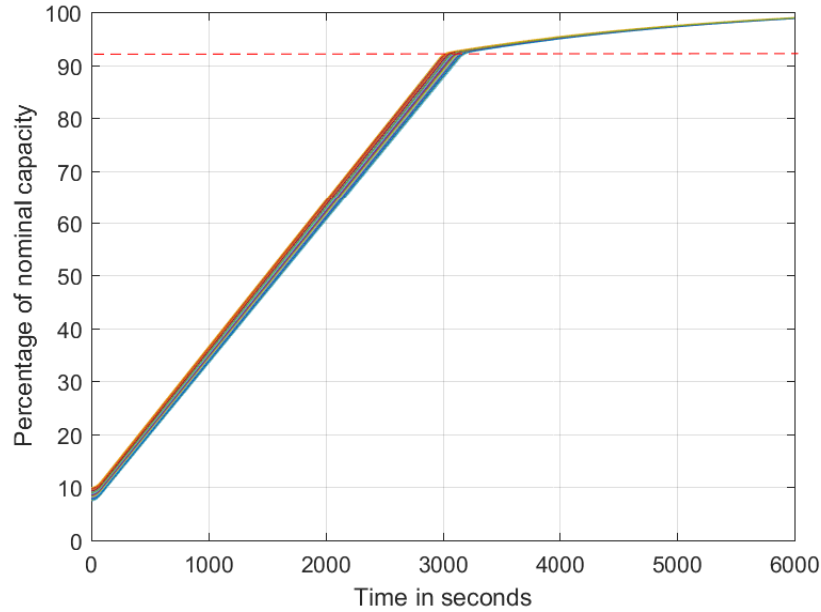


Figure 4.10: Percentage of nominal capacity of the 96 cells in autonomous cells battery pack

The transition to CV mode takes place individually when the cell reaches 4.0V (shown by the red dotted line). In comparison to the conventional cells battery pack, the transition to the CV mode is independent of the weakest cell in the battery pack. This reduces the charging time in CV mode and also leads to a better charging characteristic and a much better SoC of the cells after the charging is terminated.

4.3 Ageing of the Battery Pack

The figure below shows the current profile over 1 cycle. The plot compares the cell current of the weakest cell in autonomous and conventional cells battery pack.

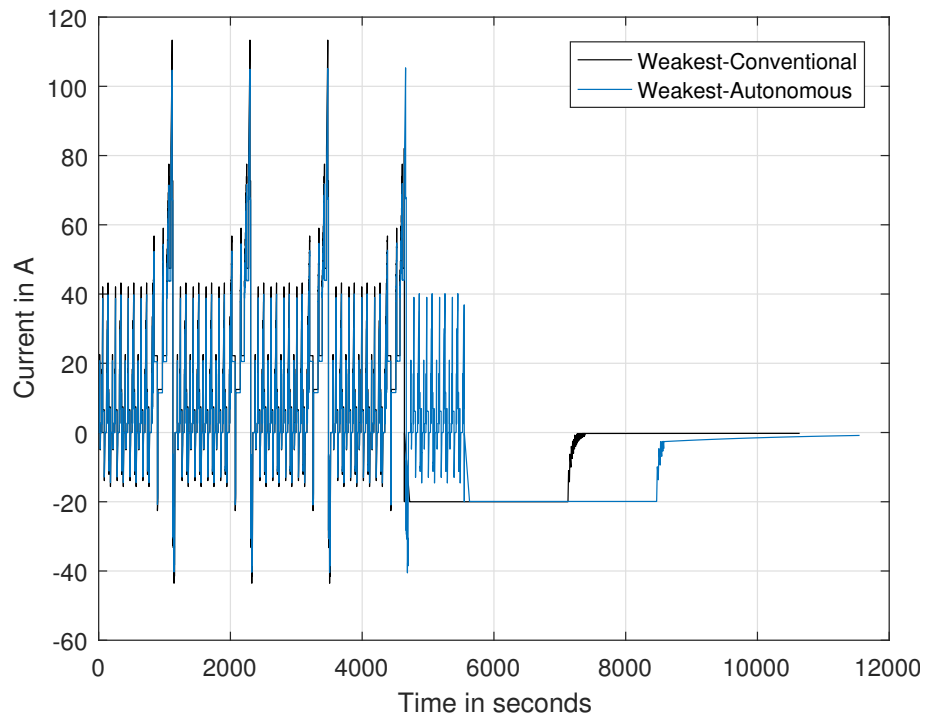


Figure 4.11: Comparison of the weakest cell current between the two systems

Figure 4.11 is magnified between 400s to 5600s to illustrate a better difference in the magnitude of the cell currents. This is shown in Figure 4.12.

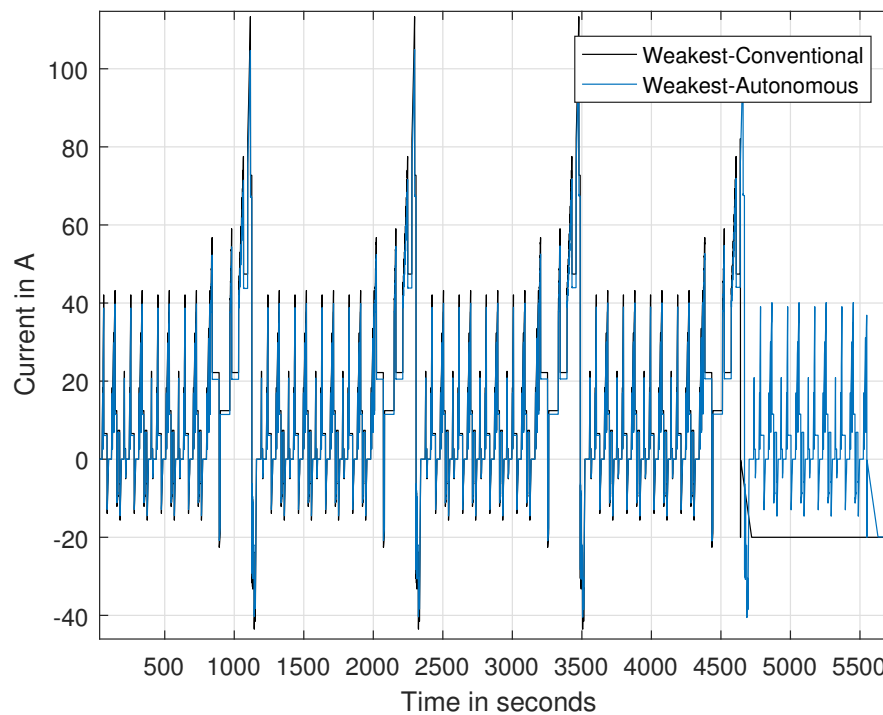


Figure 4.12: Comparison of the weakest cell current between the two systems - Magnified

It can be observed that, the magnitude of current through the weakest cell

of the conventional cells battery pack is always higher than in the weakest cell of the autonomous cells battery pack. This takes place due to the lack of load management in the conventional cells battery pack and leads to a faster ageing which has a high impact on the lifetime of the cells. As a result, the weaker cell in the conventional cells battery pack experiences a higher stress level in every cycle.

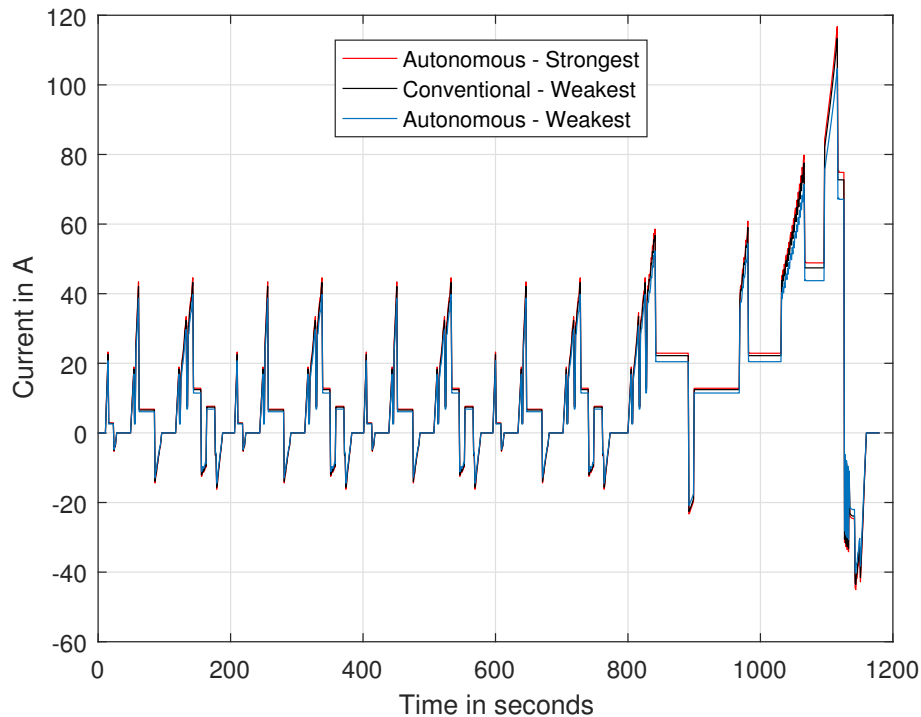


Figure 4.13: Comparison of the weakest and strongest cell currents between the the systems

The ageing rate of the weaker cell in the autonomous cells battery pack is reduced while the stronger cell carries a higher current, this leads to a faster ageing of the stronger cells. Over a period of time, the ageing rate of both the weaker and stronger cells match and thus, the pack ages uniformly. Since, the same current flows through all the cells in the conventional cells battery pack, the weaker cells become weaker and weaker as they see a net higher C-rate for the same current than the stronger cell in the conventional cells battery pack does, thus, the ageing rate is not balanced between the weaker and the stronger cells. This difference in current is shown in Figure 4.13 over 1 NEDC.

A histogram of current conveys the information on the amount of time the cell spends in various current regions over 1 cycle. To make a comparison study, the current histograms of the weakest cell in both the battery packs are plotted in the next sections.

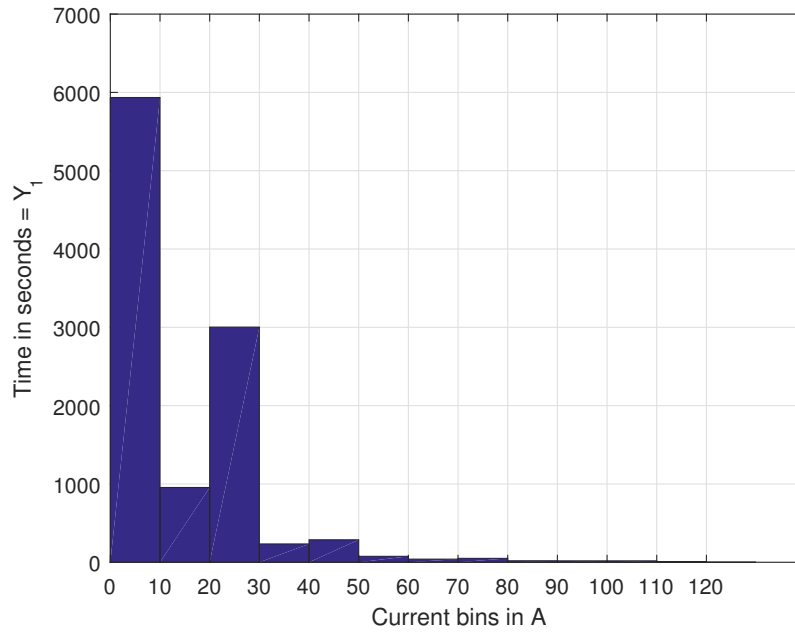


Figure 4.14: Histogram of the weakest cell current in conventional cells battery pack

Figure 4.14 is a histogram of the weakest cell current in the conventional cells battery pack over 1 cycle. The y-axis represents the time in which each of the current bins spend over this cycle. The weakest cell in the conventional cells battery pack experiences a higher magnitude of current than the weakest cell in the autonomous cells battery pack as seen in Figure 4.12. Thus, the weakest cell in the conventional cells battery pack spends longer time in the high current regions as shown in Figure 4.14.

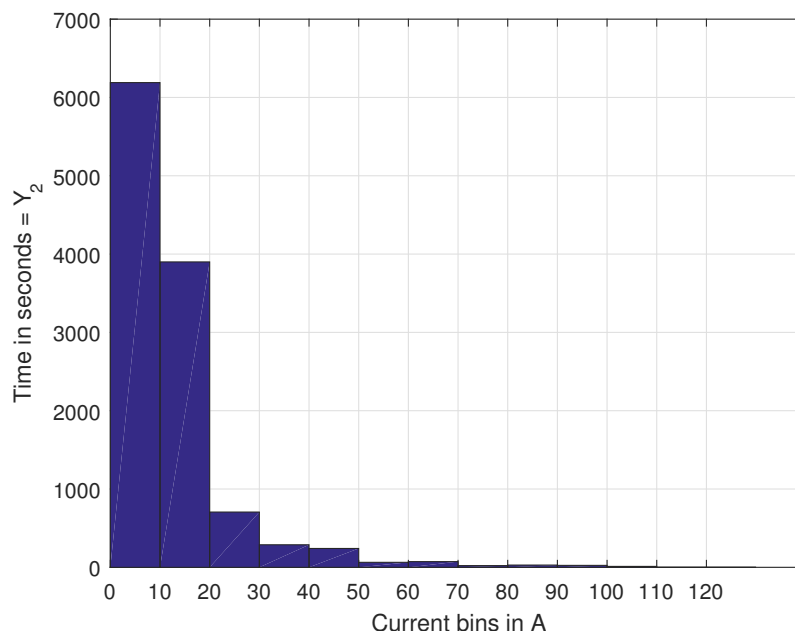


Figure 4.15: Histogram of the weakest cell current in autonomous cells battery pack

Figure 4.15 is a histogram of the weakest cell current in autonomous cells battery pack over 1 cycle. The y-axis represents the time in which each of the current bins spend over this cycle. As shown in Figure 4.12, the weakest cell in the autonomous cells battery pack has a lower magnitude of current than the weakest cell in the conventional battery pack. Thus, the weakest cell in the autonomous cells battery pack spends more time in the lower current bins as seen in Figure 4.15.

In order to protect the weaker cell, it is necessary to operate it in lower current regions for longer time. To compare the two systems better, a third histogram whose y axis represent

$$Y_{axis} = Y_2 - Y_1 \tag{4.2}$$

is plotted.

In Figures 4.16 and 4.17, a positive value of Y_{axis} means that the weakest cell in autonomous cells battery pack spends more time for that current bin and conversely, a negative value of Y_{axis} is negative means that the weakest cell in a conventional cells battery pack spends more time for that current bin. These regions are marked in the histograms below.

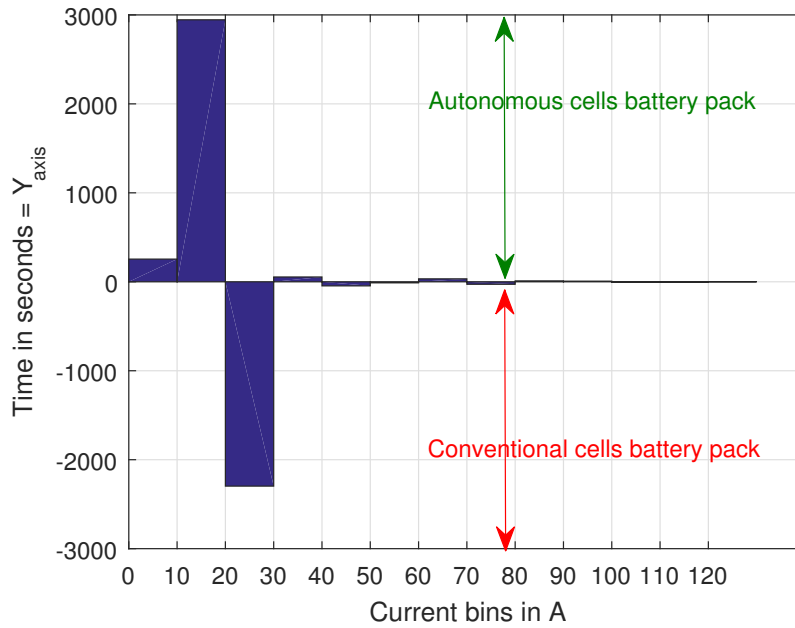


Figure 4.16: Difference in the time spent in various current regions of both the systems

From Figure 4.16, it is obvious that, the weakest cell in an autonomous cells battery pack spends more time in lower current regions.

Figure 4.17, is a magnification of Figure 4.16 at the higher values of current bins (30A to 120A) to have a better view in those regions.

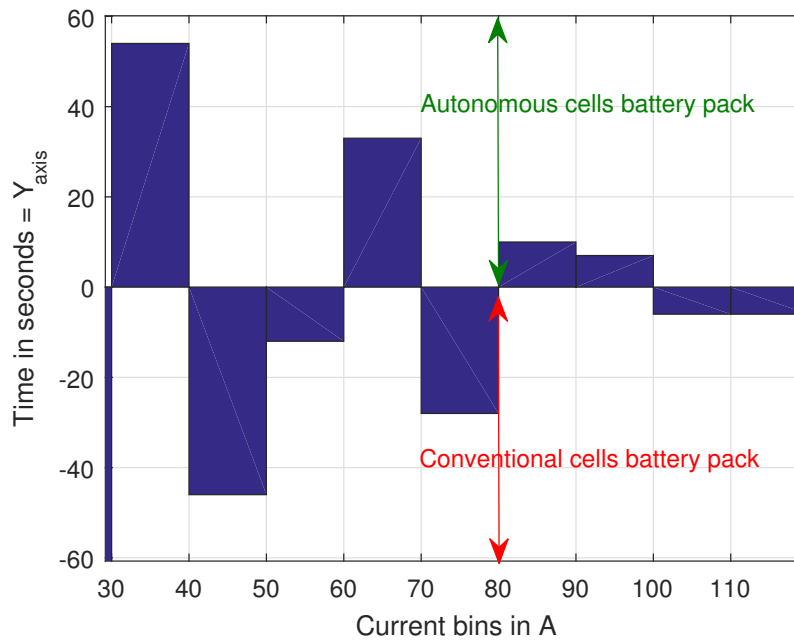


Figure 4.17: Magnified at higher current values (30A - 120A) from figure 4.16

It can be observed that the weakest cell in the autonomous cells battery pack spends less time in higher current regions.

These histograms serve as an initial identification that there can be an improvement in the pack ageing in case of autonomous cells battery pack as the weakest cell spends more time in lower current regions unlike the weakest cell in a conventional cells battery pack. A quantitative measure of improvement in ageing has to be calculated. For this, a more complex model is built and analysed.

4.3.1 Ageing Model

The results of the ageing model in this simulation is linear, thereby, it is performed only for 100 cycles and extrapolated for higher number of cycles to avoid longer waiting times during simulation. For further discussions on ageing, the characteristics of just the strongest, the median and the weakest cells are plotted and it serves two purposes:

- To ensure the strongest cell in the autonomous cells battery pack is not aged more than the weakest cell
- To act as a boundary within which the characteristics of the other cells lie. This is due to linearity in the model behavior

Thus, in all the upcoming discussions, only the strongest cell, the median cell and the weakest cell characteristics are plotted.

4.3.1.1 1C/1C Rate

The set point for the damage factor was to achieve a reduction of 10% in the initial capacity as the EOL criteria when the battery pack is cycled at 1C rate.

Conventional cells battery pack: The cell current and SoC for conventional cells is shown in figure 4.18

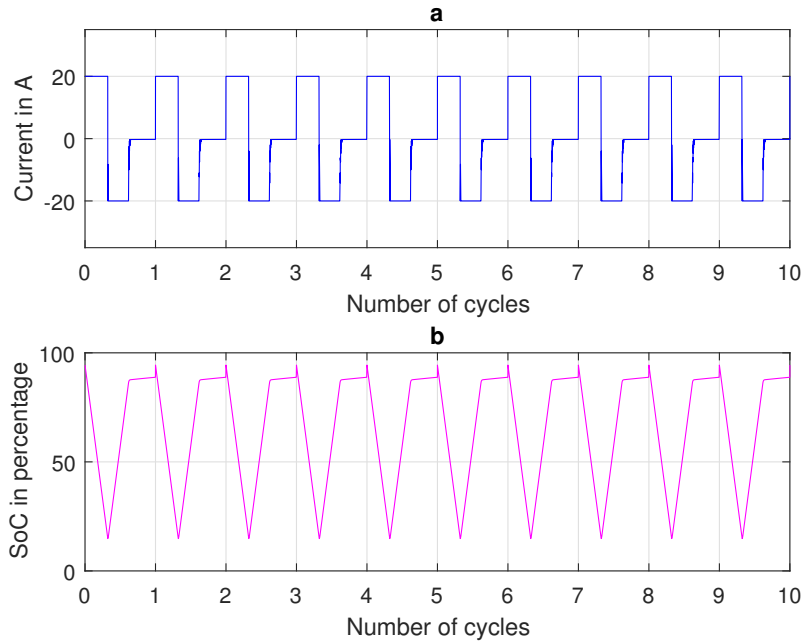


Figure 4.18: 1C cycles - Conventional cells battery pack

This current (a) and SoC profile (b) act as an input to the ageing model whose output is the ageing behaviour of the cells. These behaviour is linearised to accelerate the simulation time.

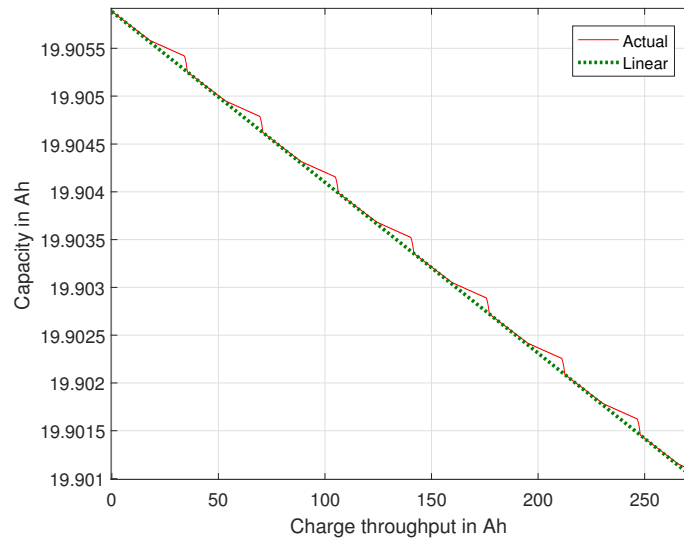


Figure 4.19: Actual and linear ageing curves

In Figure 4.19, the range of the y axis is negligible when compared to the range of the x-axis, thus, the error in the linearised curve is negligible and is accurate enough to compare the ageing behavior of the two battery packs. Linearised curves also help in achieving faster simulation times while cycling.

The base condition established was to design a damage factor curve for current and SoC (shown in Figures 3.7 and 3.8 respectively) such that the cell loses 10% of its capacity when subjected to 3000 full cycles at 1C rate. Figure 4.20 validates this calculation for conventional cells battery pack.

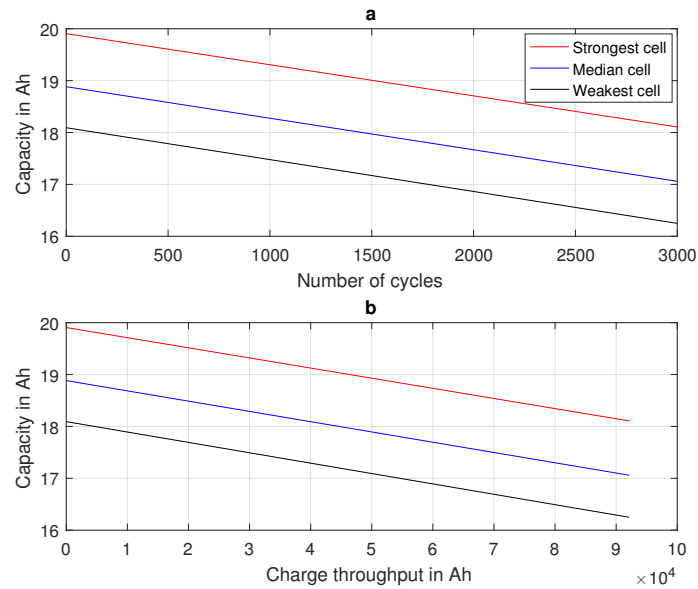


Figure 4.20: Ageing curve for 1C cycle rate - Conventional cells battery pack

In Figure 4.20 (a) represents *Capacity vs Number of cycles* and plot (b) represents *Capacity vs Charge throughput* of the 3 cells under consideration.

Here, it is observed that there is a loss of approximately 9% of the initial capacity of the median cell for 2438 cycles.

Autonomous cells battery pack: A similar cycling plot on the weakest cell is shown in figure 4.21. The current is at 1C with respect to the weakest cell capacity.

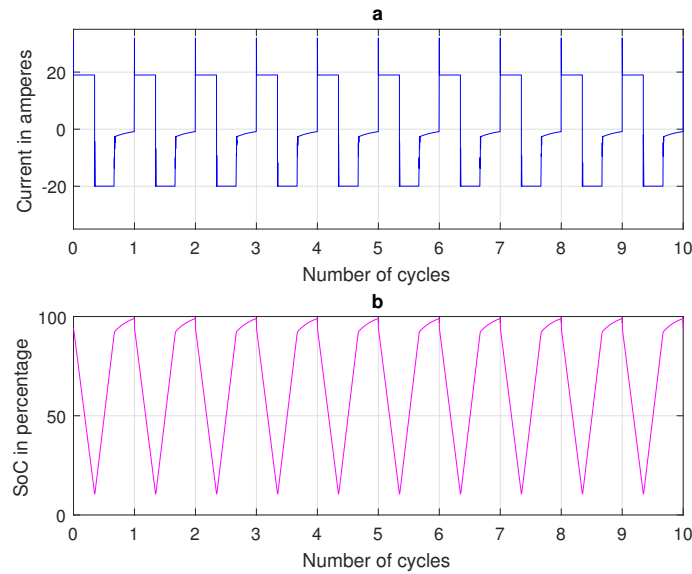


Figure 4.21: 1C cycles - Autonomous cells battery pack

In Figure 4.21 (a) represents *Capacity vs Number of cycles* and plot (b) represents *Capacity vs Charge throughput* of the 3 cells under consideration.

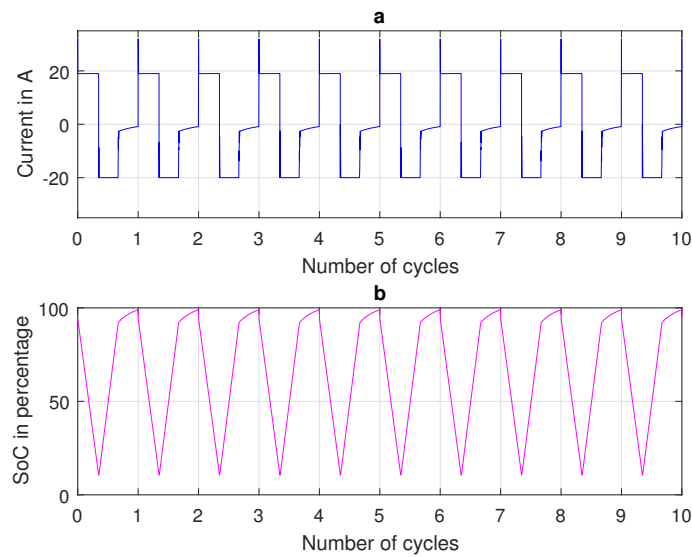


Figure 4.22: Ageing curve for 1C cycle rate - Autonomous cells battery pack

In Figure 4.22, we observe that there is a loss of approximately 9% of the initial capacity of the median cell for 2734 cycles. These results show us that the modelled system is concurrent with the designed values.

To summarize, *Capacity vs. Charge throughput* is plotted for all the 3 cells in both the battery packs in the same graph.

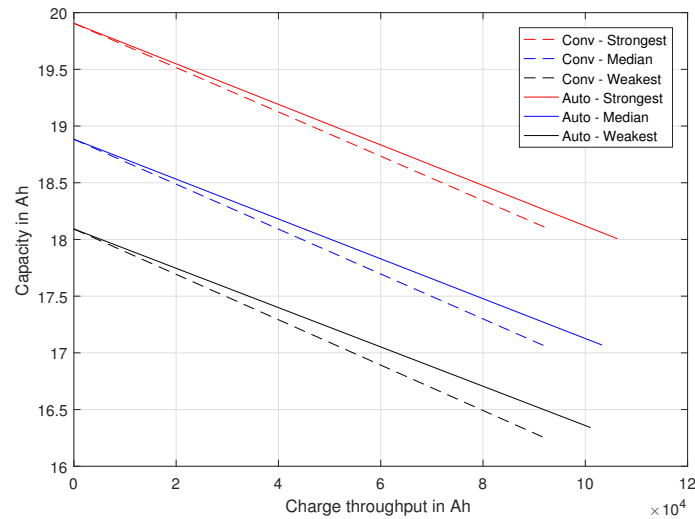


Figure 4.23: Capacity vs charge throughput - Comparison

From Figure 4.23, it is seen that the charge throughput of the autonomous cells is larger than the charge throughput of the conventional cells. The charge throughput of the weakest cell in both the battery packs are compared in the graph below.

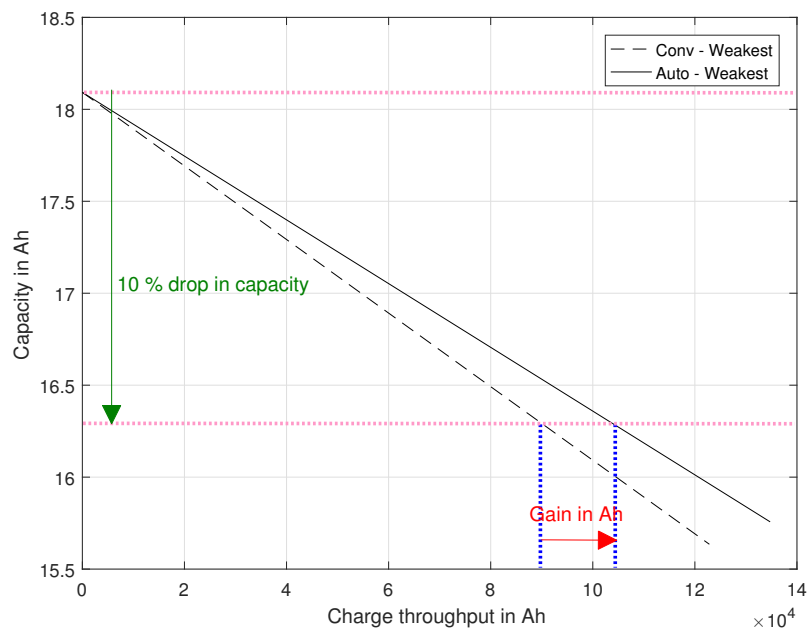


Figure 4.24: Capacity vs charge throughput - Comparison

The charge throughput of the weakest cell in the autonomous cells battery pack is higher by 1.3816×10^4 Ah, translating to 383 more cycles for the weakest cell in the autonomous cells battery pack than the conventional cells battery pack for 1C cycles.

4.3.1.2 C-Rate Determined by NEDC

Now that the base condition for both battery packs are established, it is good to proceed with further analysis where the battery packs are stressed by various currents and SoCs.

In this section, a similar analysis is made to determine the loss in the capacity of the 3 cells due to cycling, using the currents from the driving dynamics described by NEDC.

Conventional cells battery pack: Figure 4.25 shows the current and SoC profile of the weakest cell in the conventional cells battery pack subject to cycling.

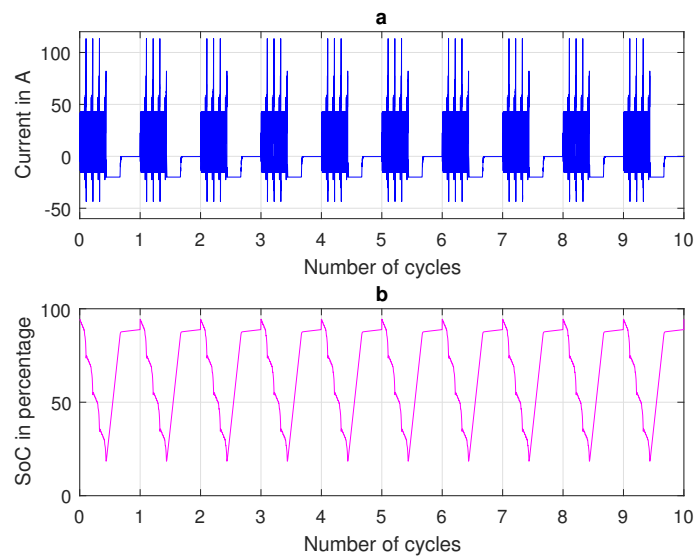


Figure 4.25: Current and SoC cycles - Conventional cells battery pack

In Figure 4.25, the strongest and the median cell have a similar characteristic but have higher magnitudes of SoC and same current profile as all the cells carry the same current.

In Figure 4.26, plot (a) represents *Capacity vs Number of cycles* and plot (b) represents *Capacity vs Charge throughput* of the 3 cells under consideration.

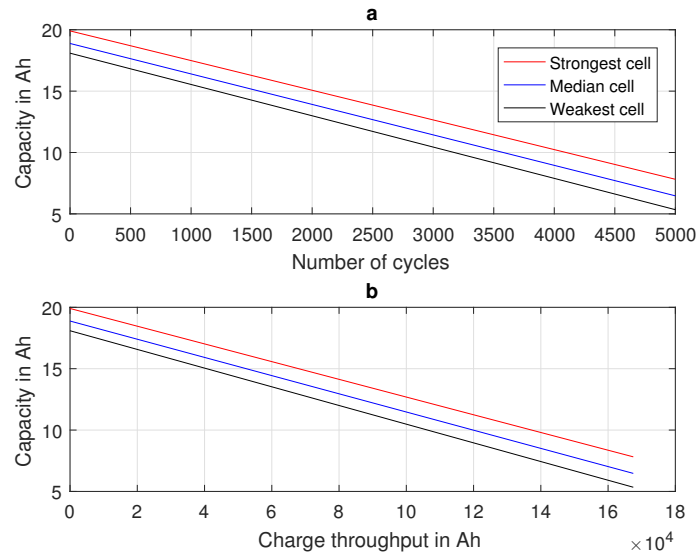


Figure 4.26: Ageing curves for conventional cells battery pack

In Figure 4.26, the decay in capacity of these 3 cells are depicted for 5000 cycles. It is clearly seen that there is no matching in ageing rates between the cells and all the cells are forced to deliver the same charge throughput (shown in Figure 4.26(b)). having all the cells deliver the same charge throughput increases the ageing rate of the weaker cells and leads to non-uniform ageing of the battery pack. Thus, the lifetime of the module or a pack depends on the lifetime of the weakest cell.

Autonomous cells battery pack: Figure 4.27 shows the current and SoC profile of the weakest cell in the conventional cells battery pack subjected to cycling. Even though the autonomous cells battery pack discharges for 909 seconds longer, (Figure 4.6) there is a significant reduction in ageing rate of the cells. This is possible due to the load management on individual cell basis.

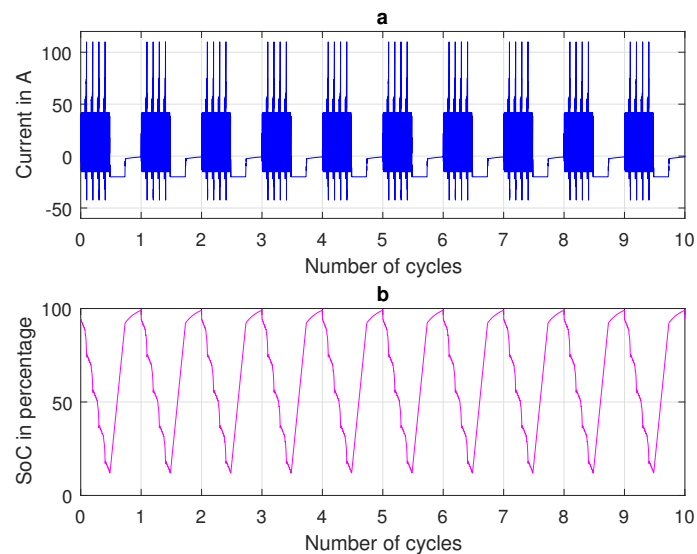


Figure 4.27: Current and SoC cycles - Autonomous cells battery pack

The strongest and the median cell have a similar characteristic of (cell

current and SoC) but has higher magnitudes of SoC and current profile as seen in Figure 4.27.

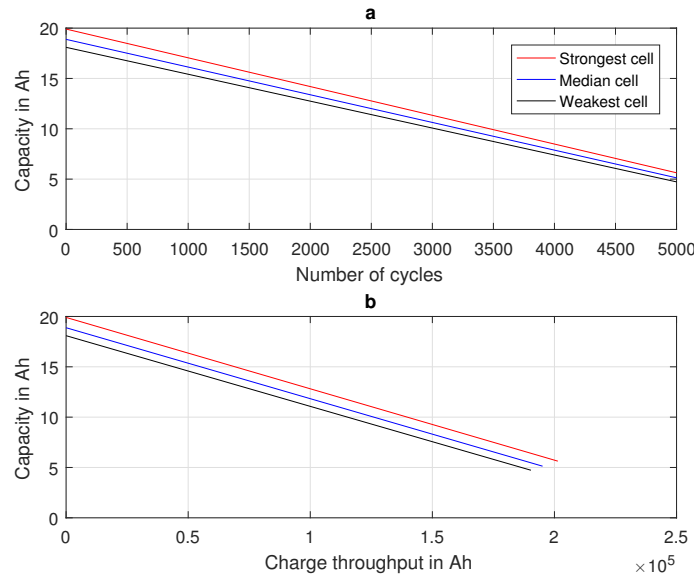


Figure 4.28: Ageing curves for Autonomous cells battery pack

The decay in the capacity of these 3 cells are depicted for 5000 cycles. A similar analysis is made as shown in Figure 4.23 and 4.24, the weakest cell in the autonomous cells battery pack yields 1981 Ah more charge throughput translating to 55 more cycles for the weakest cell in the autonomous cells battery pack than the conventional cells battery pack .

4.4 Impact of Increase in Capacity Spread of the Cells

All the results thus far, is simulated for a capacity spread with a mean (μ) of 94.99% and a standard deviation (σ) of 2.18%. Enforcing relaxed restrictions on capacity spread of cells leads to a more economical manufacturing of the battery pack, thus, it becomes crucial to analyse the behavior of the battery packs with increased capacity spread.

In the upcoming sections, a similar analysis is made on the battery packs with an increased capacity spread having a mean (μ) of 96.4% and a standard deviation of (σ) 10.13%. The impact of this capacity spread on energy output, charging characteristics and ageing is analysed.

4.4.1 Capacity fade

The graph below compares the capacity fade of both the conventional and autonomous cells battery pack system with an increased mean and standard deviation.

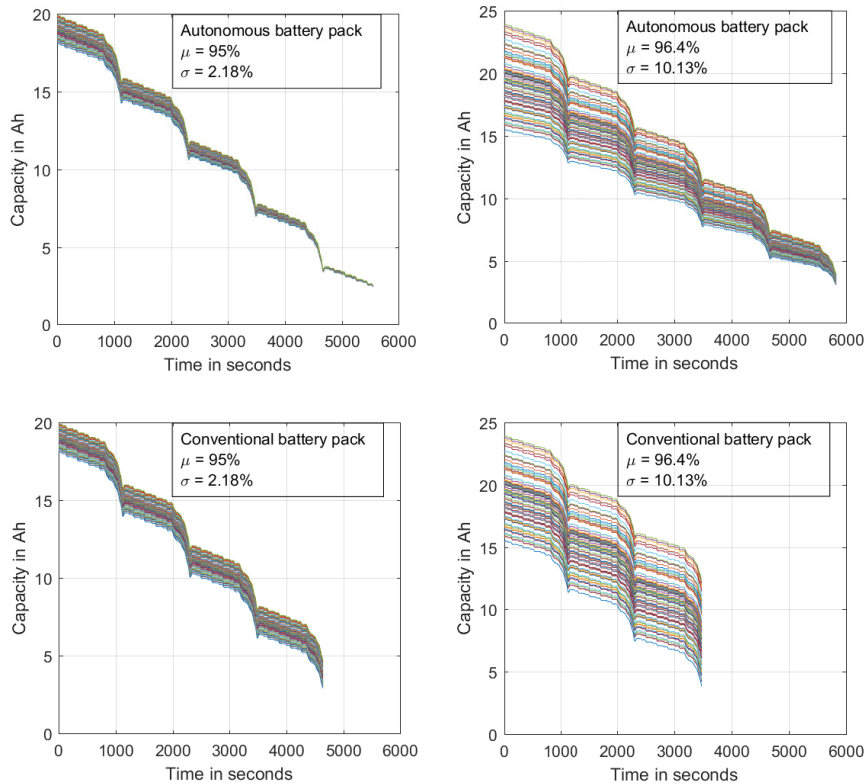


Figure 4.29: Comparison of capacity fade over a discharge cycle

Despite the fact that the standard deviation in capacity is increased from 2.18% to 10.13%, the autonomous cells battery pack is still able to supply the load for a significantly longer time than the conventional cells battery pack. In the conventional cells battery pack, there is no load management on individual cells, thus, stressing the weakest cell more and reaching the cut-off limits earlier.

It is obvious that the range of the autonomous cells battery pack is significantly higher than the conventional cells battery pack. The table below summarises these results for a better comparison.

Table 4.2: Simulated results for $\mu = 96.4\%$ and $\sigma = 10.13\%$

	Autonomous Pack	Conventional Pack
Range (<i>km</i>)	53.57	31.91
Energy Output (<i>kWh</i>)	7.52	4.47
Cut-off Time (<i>s</i>)	5823	3473
ΔV (<i>mV</i>)	18	436

The autonomous cells battery pack is found to be more advantageous even when there is a higher capacity spread.

4.4.2 Charging Characteristics

In this section, the charging characteristics of the battery packs are compared for both the spreads.

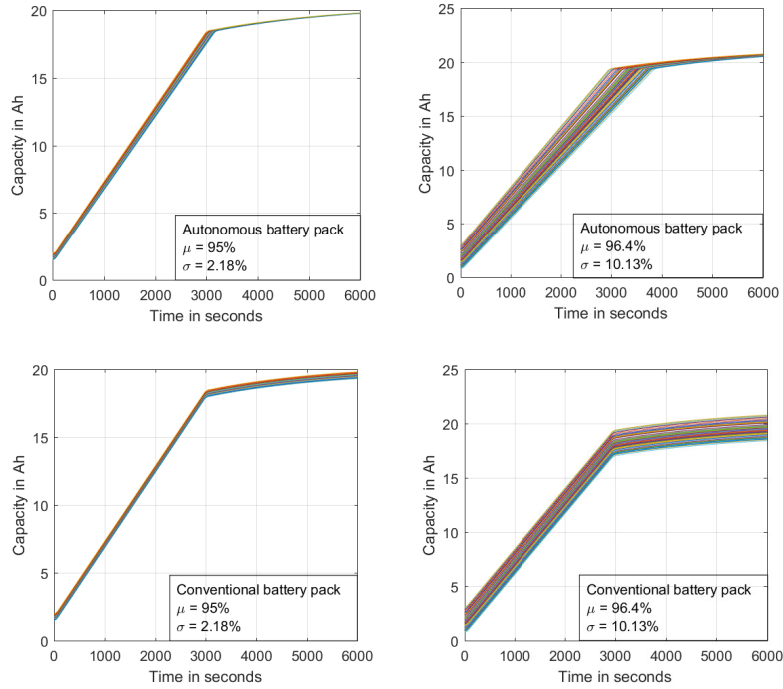


Figure 4.30: Comparison of capacity over a charge cycle

A similar behaviour is seen in the system. There is a better charging characteristic observed and the need for passive balancing circuit becomes expendable in case of autonomous cells battery pack. There exists a similar trend in CC-CV plot where each cell is charged based on its capacity.

4.4.3 Ageing

In order to have an overall behavior of the system with the increased capacity spread, just one plot of *Capacity vs Charge throughput* comprising of the 3 cell characteristics, *viz.* strongest cell, the median cell and the weakest cell for both the battery packs with the new capacity spread is plotted for the 2 scenarios in the sections below.

4.4.3.1 1C/1C Rate

The two battery packs under consideration are subjected to 1C cycles (shown in Figures 4.18 and 4.22) and the charge throughput comparison is made.

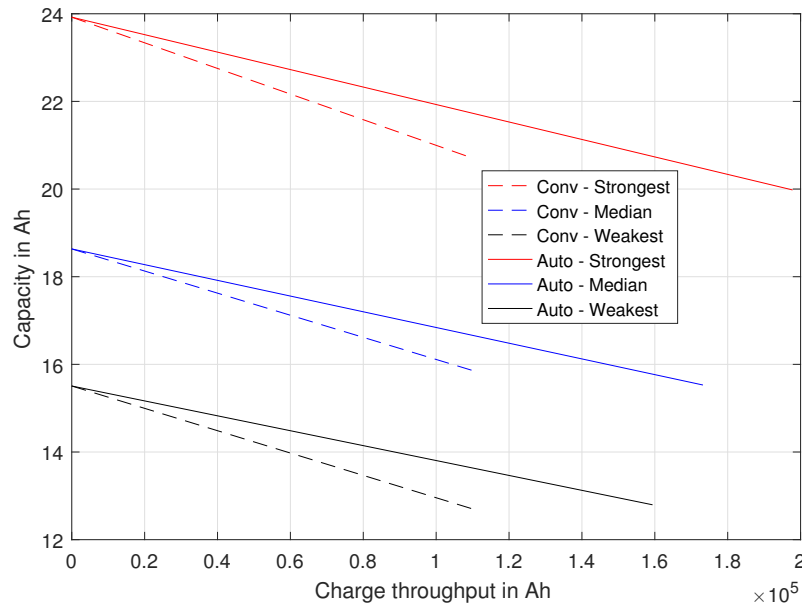


Figure 4.31: Comparison of capacity throughput - $\mu = 96.4\%$; $\sigma = 10.13\%$

From Figure 4.31 it is very evident that the cells in autonomous battery yield a higher charge throughput. There is a significant difference in the ageing rate of the cells when there is an increase in capacity spread.

Even when the capacity spread of the cells were increased, there is a gain of approximately 3.0472×10^4 Ah in case of using the autonomous cells battery pack. This translates to 983 more cycles for the weakest cell in the autonomous cells battery pack than the weakest cell in conventional cells battery pack.

4.4.3.2 C- Rate Determined by NEDC

The two battery packs under consideration are subjected to the cycles where the C-rates are determined by NEDC (shown in Figures 4.25 and 4.27) and the charge throughput comparison is made.

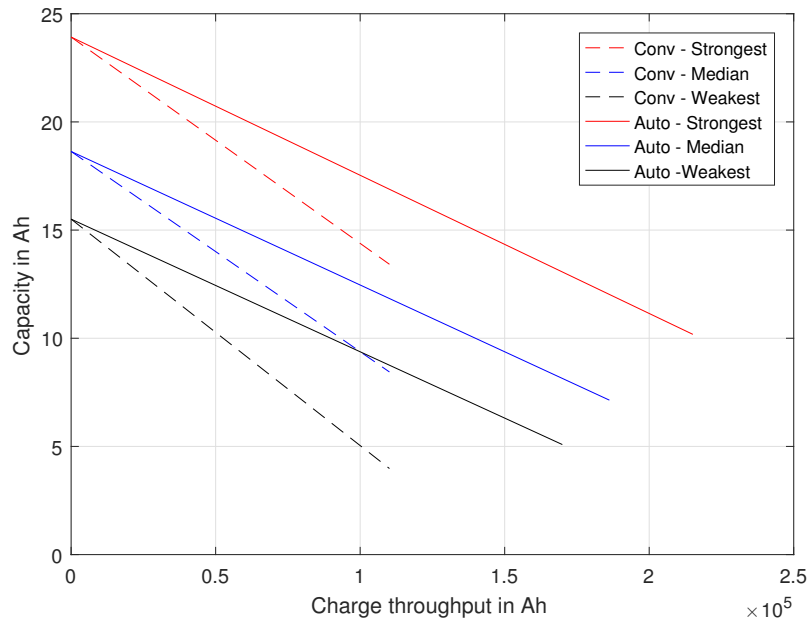


Figure 4.32: Comparison of capacity throughput - $\mu = 96.4\%$; $\sigma = 10.13\%$

From Figure 4.32 it is very evident that the cells in autonomous battery yield higher charge throughput.

It is seen that there is a gain of approximately 1.0515×10^4 Ah in case of an autonomous cells battery pack despite the fact that there was a higher capacity spread in the cells translating to 339 more cycles for the weakest cell in the autonomous cells battery pack than the weakest cell in conventional cells battery pack.

From the above analysis, it is evident that the performance of the conventional cells battery pack decreases with the increase in capacity spread. Meanwhile, the autonomous cells battery pack is found to be more susceptible to the changes in the capacity of the cells.

5

Test Cases

All the results and analysis made thus far have been based on a driving pattern obtained from the NEDC which is a standardized drive cycle therefore, it would be interesting to investigate the behaviour of both the autonomous cells battery pack and conventional cells battery pack when they are subjected to a real life driving pattern instead of a standard drive cycle. Few test cases are developed before developing a valid use case. The test case data acts as a way to evaluate the model.

Two test cases are considered *viz.* city driving and highway driving.

5.1 City Driving

City driving involves a lot of start-stop events due to higher number of vehicles on the road, pedestrians, traffic lights etc. This type of driving involves spending less time on the highway where there is a free flow of traffic without any congestion.

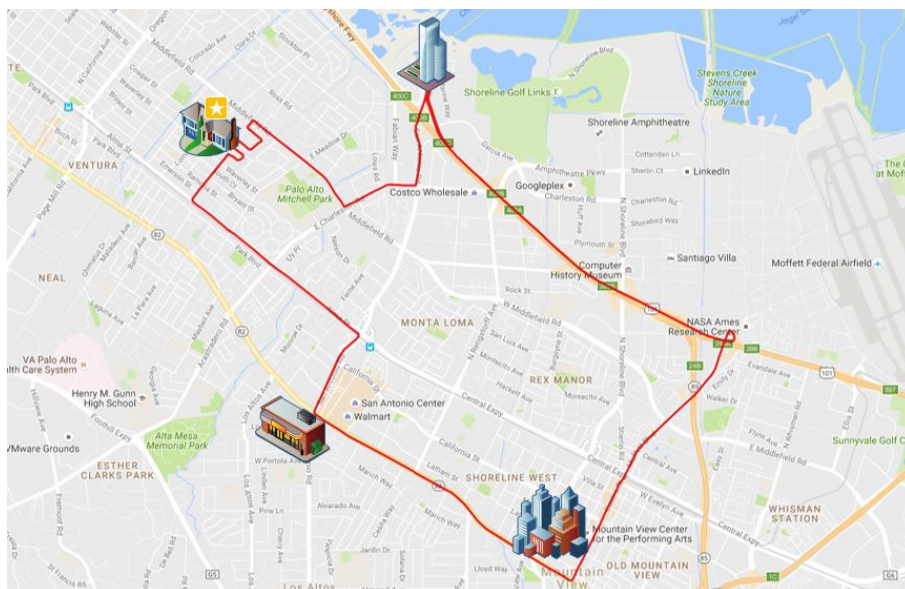


Figure 5.1: City commute under consideration - 19 km

A typical city commute involves a trip to work place from home and *vice versa*. It may also include running basic errands, grocery shopping, socializing etc. To get an actual feeling of the driving pattern during a weekday, data logging devices to monitor speed of the vehicle at a sample rate of 1 Hz were installed in a car.

The route under consideration is shown in Figure 5.1, the speed data was collected in and around Palo Alto, CA and Mountain View, CA locality.

The logged data is used as a drive cycle input to the battery pack and the range of the vehicle is computed.

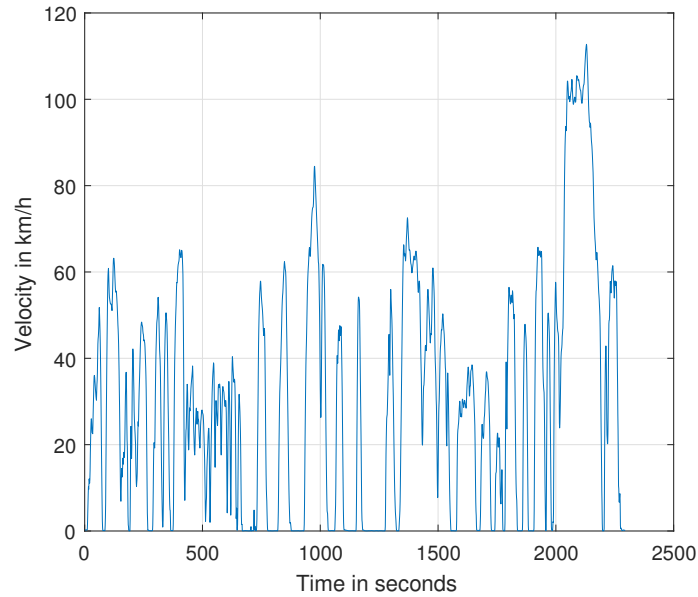


Figure 5.2: Urban driving pattern

Driving profile for the above commute is shown in Figure 5.2. Some basic characteristics of this driving pattern is summarised in the table below.

Table 5.1: Data from the city driving pattern

Characteristic	Value
Average Time per Cycle (<i>s</i>)	2296
Average Distance Travelled (<i>km</i>)	19.40
Total Energy Required (<i>kWh</i>)	2.836
Energy per <i>km</i> (<i>kWh</i>)	0.1462

The urban driving pattern is shown in Figure 5.2 is converted to equivalent electric power (*kW*) which acts as a load on the battery pack. This driving pattern is cycled till the battery pack reaches lower voltage cut-off limit and the range in both the battery packs is calculated and summarised in the table below.

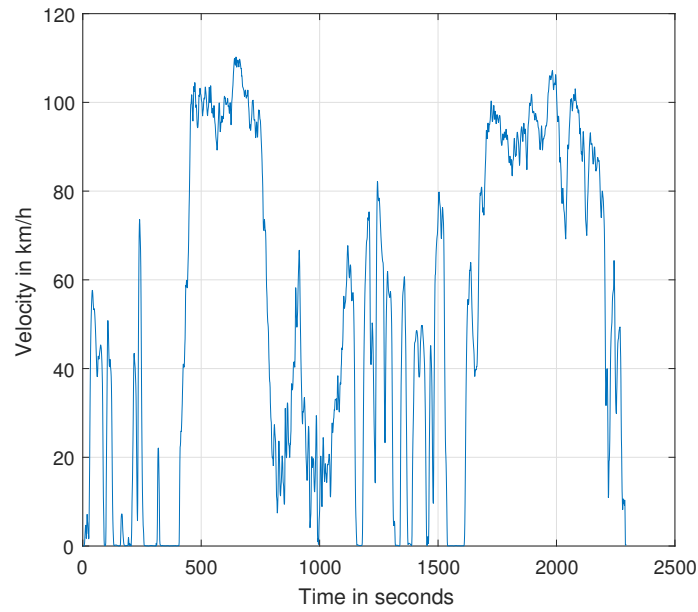


Figure 5.4: Freeway driving pattern

In Figure 5.4, the highway driving pattern is shown. Some of its characteristics is summarised in Table 5.3 below.

Table 5.3: Data from the highway driving pattern

Characteristic	Value
Average Time per Cycle (<i>s</i>)	2295
Average Distance Travelled (<i>km</i>)	33.34
Total Energy Required (<i>kWh</i>)	5.45
Energy per <i>km</i> (<i>kWh</i>)	0.164

The battery packs are cycled till the pack reaches lower voltage cut-off limit and the range in both the battery packs are calculated and summarised in the table below.

Table 5.4: Comparison - Highway driving

	Autonomous Pack	Conventional Pack
Range (<i>km</i>)	34.61	34.58
Energy Output (<i>kWh</i>)	5.80	5.63
Cut-off Time (<i>s</i>)	2531	2529
ΔV (<i>mV</i>)	2.3	104

The designed model is found to perform well even for the actual driving profile. This acts as a gateway to evaluate the use case in the next chapter.

6

Use Cases

As a tangible use case, the modelled battery packs are considered to be a part of a PHEV. The main purpose is to provide the consumer with a simple information proving the advantages in using the autonomous cells battery pack. This is done by calculating the percentage electric *km* that is driven over a commute and also by simulating and comparing ageing behavior of the two battery packs.

6.1 Percentage Electric Miles

The commute under consideration involves acquisition of velocity (*km/h*) of the car at a sample rate of 1 *Hz*. This represents the city driving conditions where, the total distance per weekday commute considered is roughly 67 *km*.

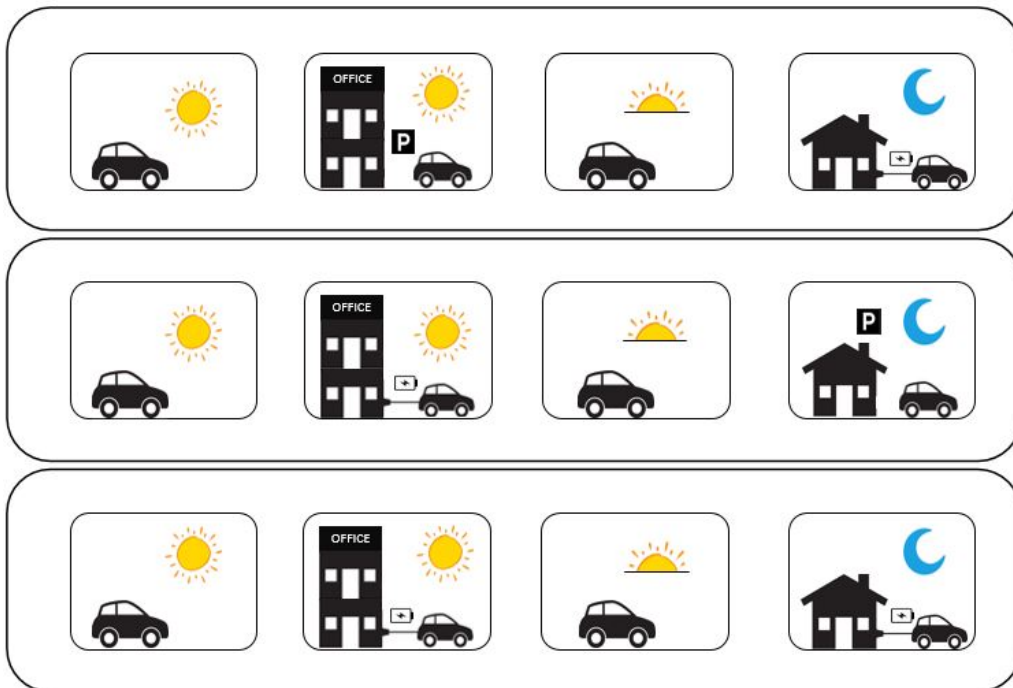


Figure 6.1: Use cases under consideration - Overview

Figure 6.1 represent the three situations classified based upon the charging of the car.

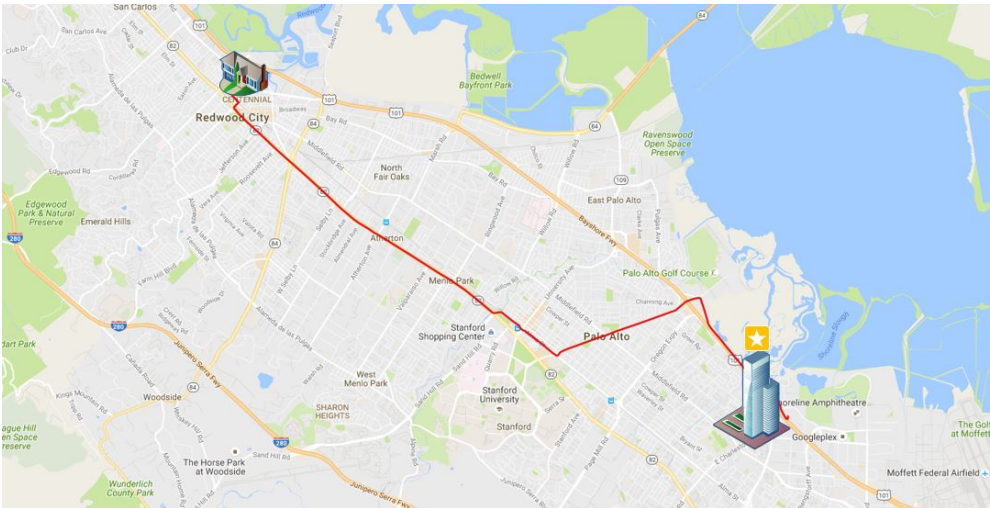


Figure 6.3: Evening commute from workplace to home - 17 km

The velocity of the car for the above commutes shown in Figures 6.2 and 6.3 is logged for the three described cases and it acts as an input for both the modelled systems.

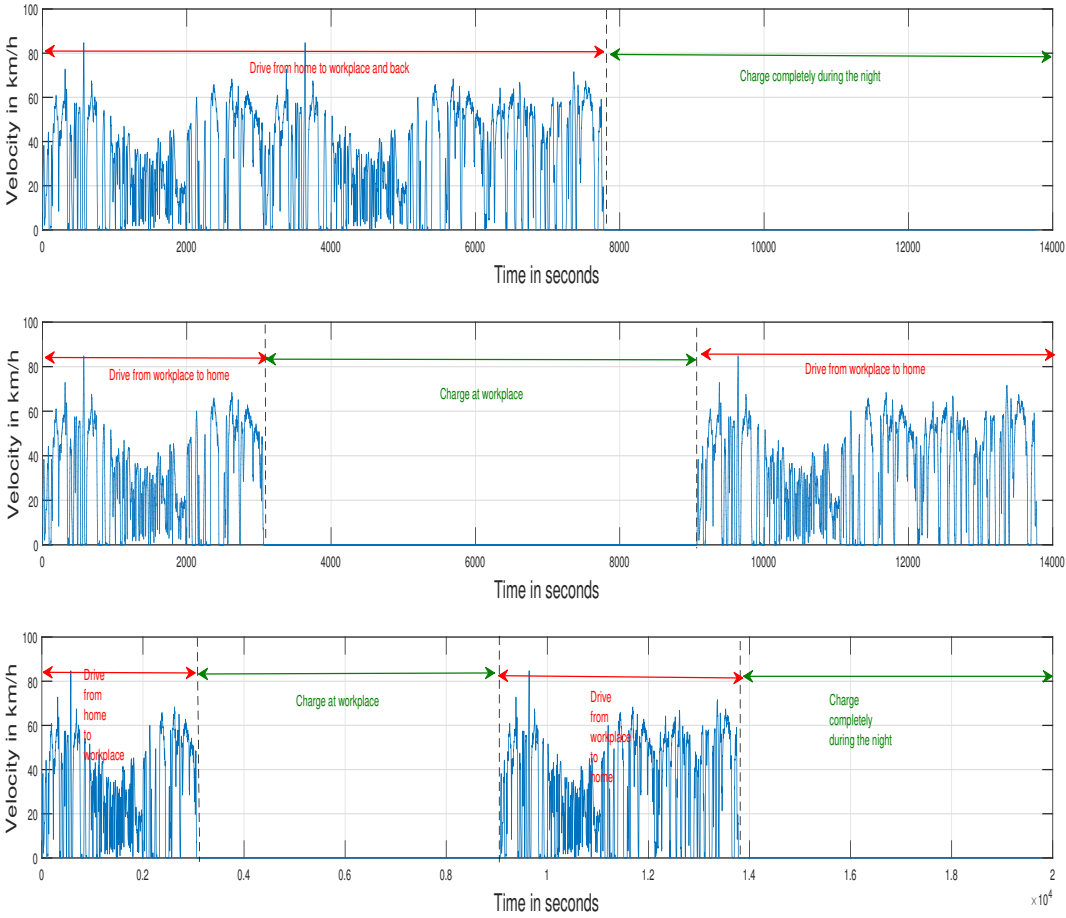


Figure 6.4: Velocities of the use cases under consideration -From top to bottom: Home charging, Workplace charging, Home and workplace charging

Figure 6.4 shows the driving profile for the three use cases under consideration. The regions with the red arrows represent discharge event and the region with green arrows represent charging event.

Table 6.1: Comparison of the electric range (km) of a PHEV for different use cases

Use Case	Autonomous Pack	Conventional Pack
Home Charging	49.8	43.2
Workplace Charging	46.9	44.9
Home and Workplace Charging	>67 *	>67 *

* The PHEV will have a full range after every charge event. In this case, both the battery packs have a range greater than 25 km which is enough to reach the workplace during the morning and when fully charged at the workplace, both the packs have the range greater than 42 km . The full range of the battery is known only when it is completely depleted

The full range (km) of the completely charged PHEV in all the 3 cases are summarised in Table 6.1. The full range is also computed with the increased capacity spread which will be summarised in the later sections. With these use cases, the percentage electric distance is calculated by

$$P_{electric} = \frac{D_{Range}}{D_{Total}} \times 100\% \quad (6.1)$$

where, $P_{electric}$ is the percentage electric distance travelled per day, D_{Range} is the range of the battery pack under consideration in km , D_{Total} is the total distance travelled in one weekday in km .

Table 6.2 summarises the percentage electric commute when using the autonomous cells battery pack and the conventional cells battery pack. It is assumed that the recuperation does not occur when the car is running on gasoline after completely discharging the battery pack.

Table 6.2: Comparison of percentage electric km driven for different use cases

Use Case	Autonomous Pack	Conventional Pack
Home Charging	74.33	64.48
Workplace Charging	70	67
Home and Workplace Charging	>100 *	>100 *

* Since the range is above 67 km , the percentage electric miles driven is also above 100.

It is seen that, in case of home charging, the PHEV with autonomous cells battery pack yields approximately 11% more electric range than a PHEV with conventional cells battery pack. In case of workplace charging, the PHEV with autonomous cells battery pack yields approximately 3% more electric range than a PHEV with conventional cells battery pack. Since the commute to workplace and the commute to home is less than the range of the battery pack, both the PHEVs run fully electric when it is charged at home and workplace.

Tables 6.3 and 6.4 compare the electric range of the battery packs under consideration for normal capacity spread ($\sigma = 2.18\%$) and an increased capacity spread ($\sigma = 10.13\%$).

Table 6.3: Comparison of range (km) - $\sigma = 2.18\%$

Load on the Electric Powertrain	$\sigma = 2.18\%$		
	Autonomous Battery Pack	Conventional Battery Pack	Percentage increase in range
NEDC	48.29	42.47	13.65
Home Charging	49.8	43.2	15.28
Workplace Charging	46.9	44.9	4.50
Home and Workplace Charging	Battery is not completely depleted to know the full range		

Table 6.4: Comparison of range (km) - $\sigma = 10.13\%$

Load on the Electric Powertrain	$\sigma = 10.13\%$		
	Autonomous Battery Pack	Conventional Battery Pack	Percentage increase in range
NEDC	53.57	31.2	69.13
Home Charging	57.35	37.38	53.42
Workplace Charging	57.25	36.46	57.07
Home and Workplace Charging	Battery is not completely depleted to know the full range		

From the above analysis we can see that there is a gain in the range when the autonomous cells battery pack is used.

6.2 Ageing

In this section, the ageing of the battery pack in both the PHEVs for all the three use cases are compared. The battery pack ageing model is cycled with the current and SoC obtained by these driving profiles. Graphs below consists of the ageing characteristics of the strongest cell, the median cell and the weakest cell in both the battery packs when it is subjected to 2500 cycles. It also shows the gain in charge throughput of the weakest cell for 10% drop in capacity in both the battery packs.

- **Home charging:**

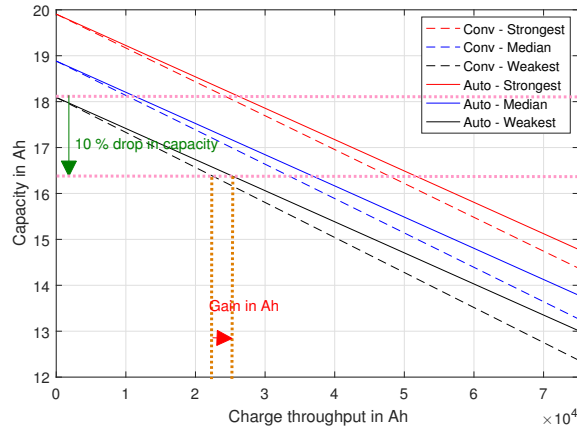


Figure 6.5: *Capacity vs Charge throughput* comparison - Home charging

Figure 6.5 shows a gain of 2968 Ah in the charge throughput of the weakest cell in the autonomous cells battery pack, translating to a cycle gain of 82.

- **Workplace charging:**

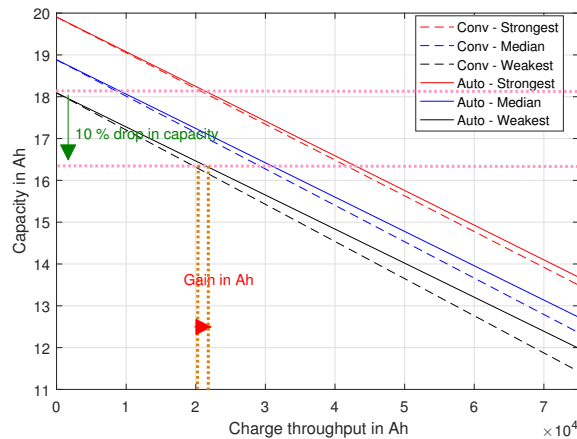


Figure 6.6: *Capacity vs Charge throughput* comparison - Workplace charging

Figure 6.6 shows that there is gain of 1834 Ah in the charge throughput of the weakest cell in the autonomous cells battery pack, yielding to 51 cycles more than the weakest cell in the conventional cells battery pack.

- Home and workplace charging:

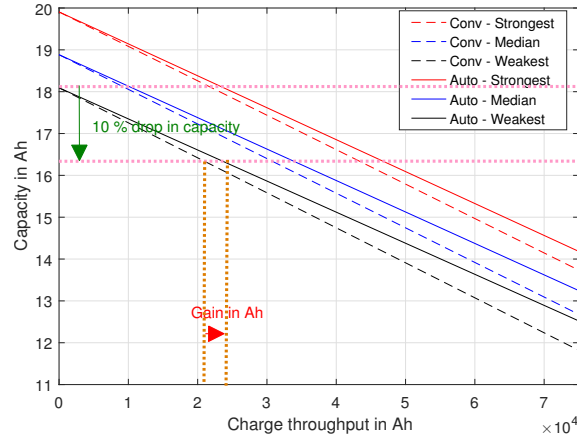


Figure 6.7: Capacity vs Charge throughput comparison - Home and workplace charging

Figure 6.7 shows that there is gain of 2700 Ah in the charge throughput of the weakest cell in the autonomous cells battery pack, yielding to 75 cycles more than the weakest cell in the conventional cells battery pack. A similar analysis is made for the increased capacity spread ($\sigma = 10.13\%$) and the results are presented in the form of Table 6.5 and Table 6.6.

From the above discussions, it is clearly seen that there is a gain in the charge throughput on the weakest cell in the autonomous cells battery pack. All these results are brought together in the form of two tables below, where the results are focused on the weakest cells in both the battery packs.

Table 6.5: Ageing summary for various earlier described loads on the electric powertrain, $\sigma = 2.18\%$ and EOL criteria = 10% drop in capacity of the weakest cell

Load on the Electric Powertain	$\sigma = 2.18\%$, Initial Capacity = 18.09 Ah						
	Autonomous battery pack		Conventional battery pack		Difference		Percentage increase in capacity
	Capacity (kAh)	Cycles	Capacity (kAh)	Cycles	Capacity (kAh)	Cycles	
1C/1C	103.4	2858	89.5	2475	13.9	383	15.47
NEDC	25.5	706	23.5	651	2.0	55	8.45
Home Charging	26.5	732	23.4	650	3.1	82	12.62
Workplace Charging	22.0	609	20.2	558	1.8	51	9.14
Home and Workplace Charging	24.1	667	21.4	592	2.7	75	12.67

Table 6.6: Ageing summary for various earlier described loads on the electric powertrain, $\sigma = 10.13\%$ and EOL criteria = 10% drop in capacity of the weakest cell

Load on the Electric Powertain	$\sigma = 10.13\%$, Initial Capacity = 15.505 Ah						
	Autonomous battery pack		Conventional battery pack		Difference		Percentage increase in capacity
	Capacity (kAh)	Cycles	Capacity (kAh)	Cycles	Capacity (kAh)	Cycles	
1C/1C	91.5	2951	61.0	1968	30.5	983	49.95
NEDC	25.4	819	14.9	480	10.5	339	70.63
Home Charging	25.5	822	16.3	527	9.2	295	55.98
Workplace Charging	20.9	674	14.7	474	6.2	200	42.19
Home and Workplace Charging	20.6	665	15.0	484	5.6	181	37.40

From the above tables, it can be inferred that a slower ageing rate is observed while using the autonomous cells battery pack. Thus, the advantages in range and ageing is observed significantly when the autonomous cells battery pack is used.

7

Conclusion

A conventional cells battery pack and an autonomous cells battery pack is compared and contrasted against various attributes as discussed in the previous sections. This section deals with a detailed conclusion along with the possible areas of further research.

Few of the crucial attributes of a battery pack *viz.* energy output, charging time, and ageing of the pack are examined. Even though there are losses in the DC-DC converter, the performance of the autonomous cells battery pack is better as opposed to the conventional cells battery pack. Conclusions drawn for each of these attributes are discussed in the following sections.

- **Range:** The autonomous cells battery pack yields more energy output, leading to more range of the EV. This is illustrated in Figure 7.1.

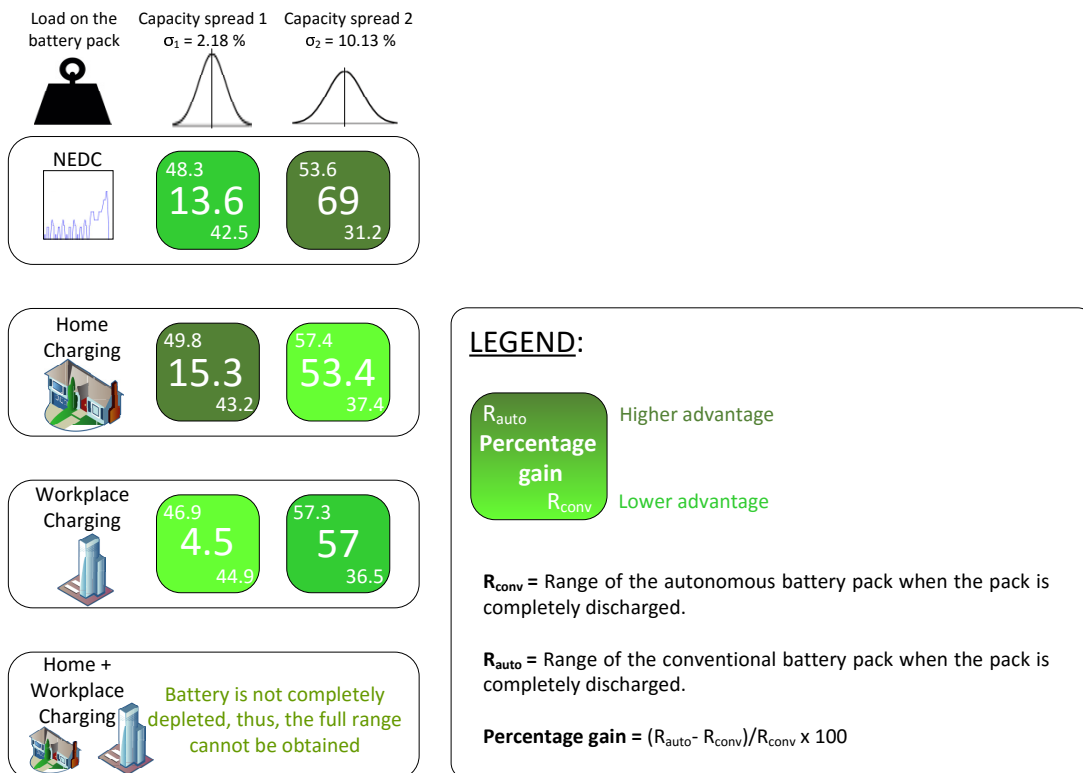


Figure 7.1: Range (km) of the battery packs under consideration for different driving profiles

There is a general trend of increase in the range when using autonomous cells battery pack. This is shown by different green icons. The darker the shade of green, the higher is the percentage increase in the range and the lighter the shade of green, lower is the percentage increase in the range. It is also observed that, with the increased capacity spread of the cells, the percentage increase in the range is higher. This is due to the load management algorithm on the individual cell level which makes the autonomous cells battery pack passive to the changes in the capacity spread.

- **Charging characteristics:** In the autonomous cells battery pack, the transition to CV mode occur on an individual cell level unlike the conventional cells battery pack where the transition to CV mode occur on a pack/module level which is determined by the weakest cell. The weakest cell in the conventional cells battery pack inhibits the charging of the stronger cells in CC mode. The DC-DC converters present in the autonomous cells battery pack acts as an active balancing device which ensures uniform charging of all the cells in the battery pack where as, the conventional cells battery pack requires a passive cell balancing circuitry which is usually bulky, inefficient and slow.

- **Ageing:** When the ageing topics are discussed, the focus is always laid on the weakest cell as it is more vulnerable to ageing, thus, bringing the battery pack performance down. The illustration below shows the situation where the weakest cell parameters are calculated. In Figure 7.2, the darker the shade of green, the higher is the percentage increase in cycles and the lighter the shade of green, the lower is the percentage increase in cycles. It becomes clear that the percentage increase in the cycles are higher when there is a higher capacity spread. This also proves that the DC-DC converters make the battery pack immune to the changes to the capacity spread.

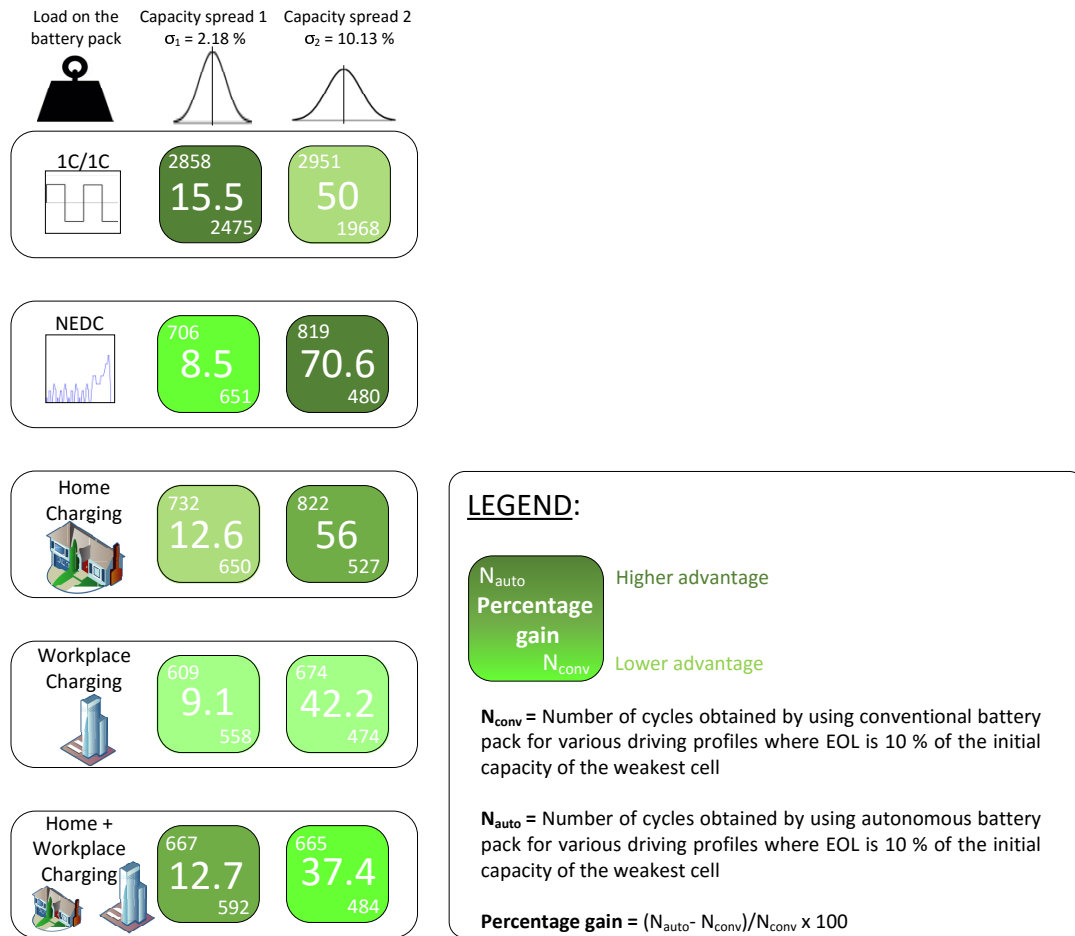


Figure 7.2: Percentage increase in ageing of the battery packs under consideration for different driving profiles

In conclusion, when the capacity spread of the cells are less ($\sigma = 2.18\%$), autonomous cells battery pack yields a better performance than the conventional cells battery pack. With the increase in the capacity spread of the cells ($\sigma = 10.13\%$), the performance of the conventional cells battery pack reduces drastically while the performance of the autonomous cells battery pack increases significantly.

8

Future Work

The DC-DC converters on the individual cells can be utilized for various applications. At present, the isolation of a faulty cell in a module is a challenging task to achieve. A single faulty cell in the module potentially destroys the entire module making it unsafe to use. The feasibility of isolation of the faulty cell in the module will be a task to examine, which poses economical and environmental benefits.

The faulty cell replacement can be seen as a modular concept, facilitating the user to unstack and stack the cells as compared to the books on the shelf in the racks. The capacity and ageing of the new cell can be adapted to the capacity of older cells in the module, making the module more versatile in the near future. The concept of modularity of the battery pack is a crucial area to perform further investigations.

The ideal temperature that the Li-ion cells like to operate is from 20 °C to 45 °C. The performance of the cell reduces above or below this specified temperature range. The DC-DC converter can be switched with various frequencies depending on the ambient temperature of the pack which induces switching losses in the system and thus, slowly heating the cells when they are at lower temperature which is an area of interest I would like to further investigate.

The autonomous cells technology, can not only be limited to battery first life in an EV, but also helps in gaining advantages in a battery second life application. Stationary energy storage to support the grid is a very typical proposed second life application, where, the load is more static and pre-determined. The cells in the battery pack will potentially see the same advantages as it does in its first life applications, but it would be interesting to see the behavior of the system where the load fluctuation is not so dynamic as it is in an EV.

A

Appendix

A.1 Conventional Cells Battery Pack

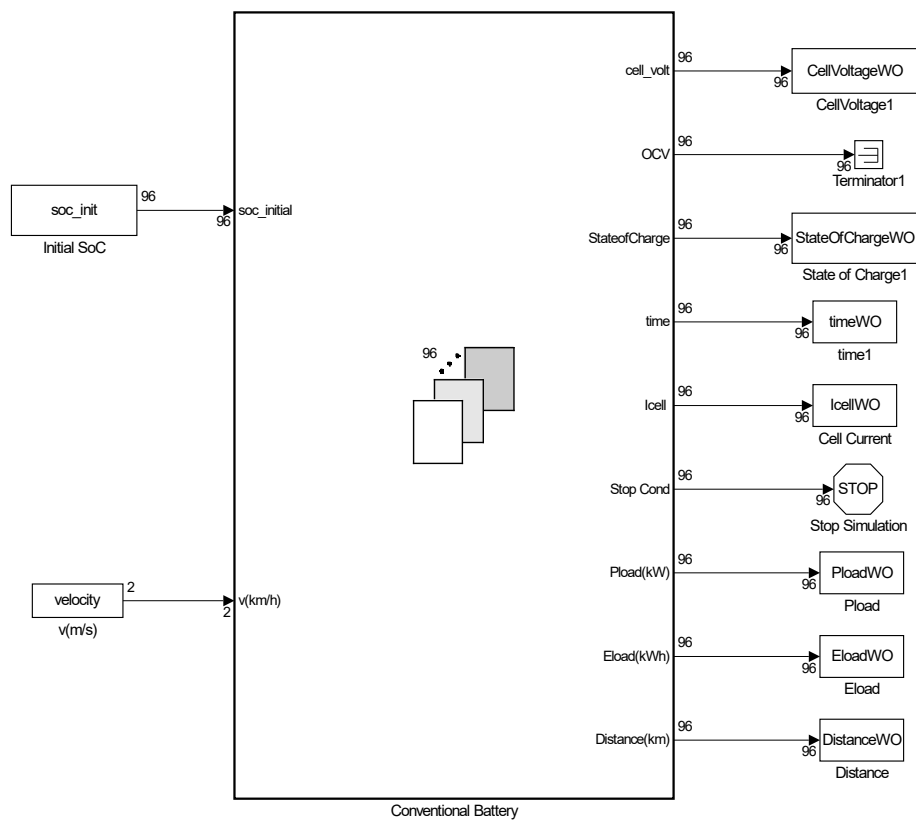


Figure A.1: Overview of the conventional cells battery pack in Simulink

A. Appendix

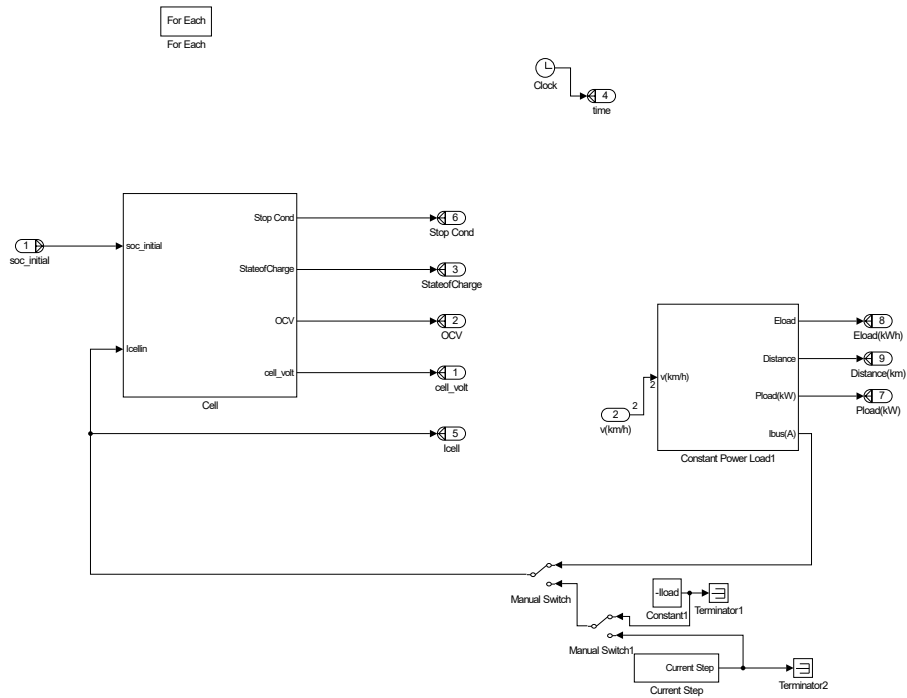


Figure A.2: Conventional cells battery pack and its components in Simulink

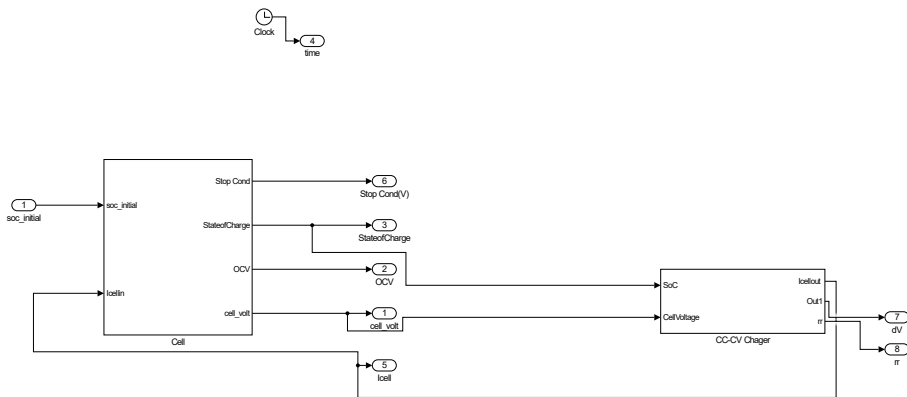


Figure A.3: Charging model of the conventional cells battery pack

A.2 Autonomous Cells Battery Pack

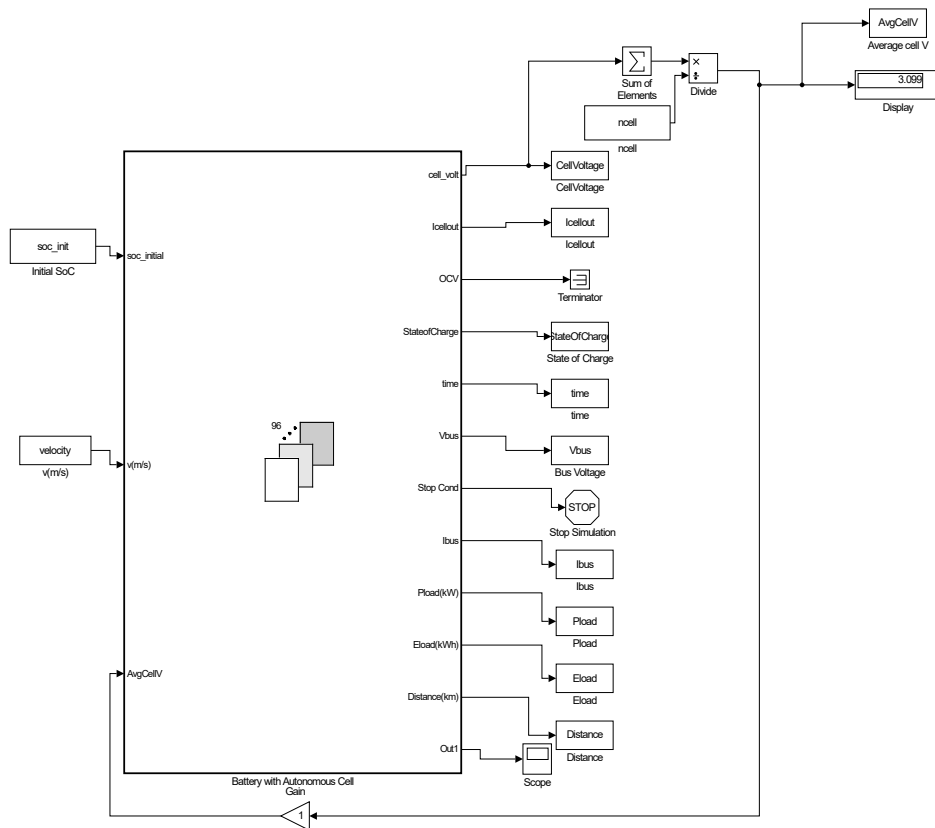


Figure A.4: Overview of the autonomous cells battery pack in Simulink

A.3 Ageing Model

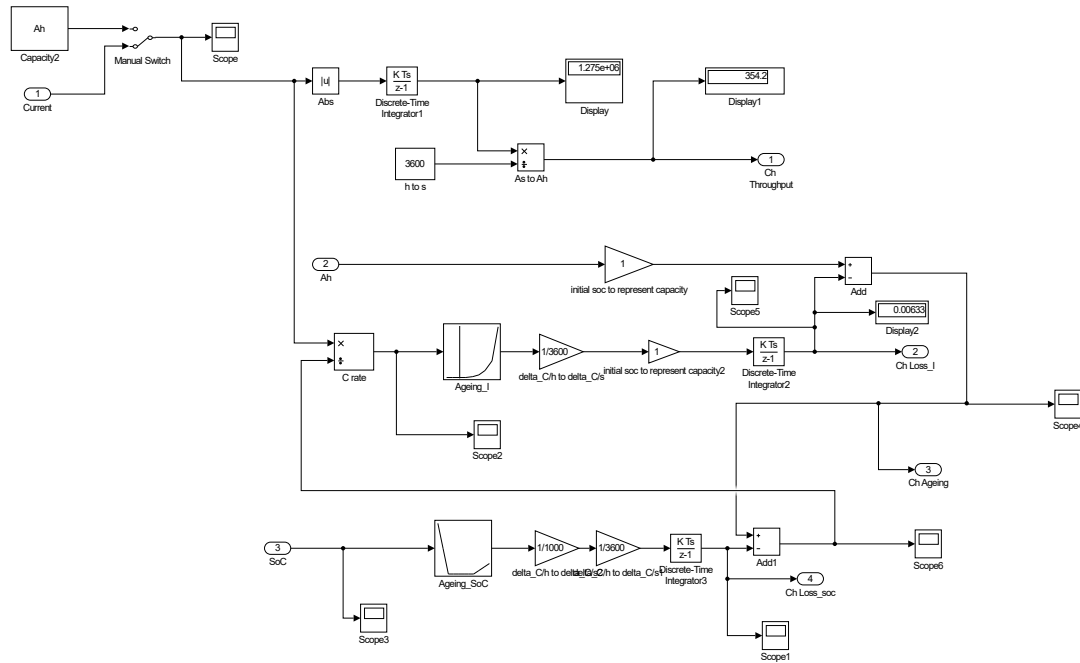


Figure A.7: Ageing model designed in the Simulink environment

Bibliography

- [1] *EPA Sets Tier 3 Motor Vehicle Emission and Fuel Standards*. <https://www3.epa.gov/otaq/documents/tier3/420f14009.pdf>.
- [2] Asif Faiz, Christopher S Weaver, and Michael P Walsh. *Air pollution from motor vehicles: standards and technologies for controlling emissions*. World Bank Publications, 1996.
- [3] AN IJESD. “Costs of lithium-ion batteries for vehicles”. In: (2000).
- [4] Davide Andrea et al. *Battery management systems for large lithium-ion battery packs*. English. 1st ed. Boston: Artech House, 2010. ISBN: 9781608071043;1608071049;
- [5] Simon F. Schuster et al. “Lithium-ion cell-to-cell variation during battery electric vehicle operation”. English. In: *Journal of Power Sources* 297 (2015), pp. 242–251.
- [6] Donghwa Shin, Enrico Macii, and Massimo Poncino. “Statistical Battery Models and Variation-Aware Battery Management”. English. In: ACM, 2014, pp. 1–6. ISBN: 9781450327305;1450327303;
- [7] Matthieu Dubarry, Nicolas Vuillaume, and Bor Y. Liaw. “Origins and accommodation of cell variations in Li-ion battery pack modeling”. English. In: *International Journal of Energy Research* 34.2 (2010), pp. 216–231.
- [8] Shriram Santhanagopalan and Ralph E. White. “Quantifying Cell-to-Cell Variations in Lithium Ion Batteries”. English. In: *International Journal of Electrochemistry* 2012 (2012), pp. 1–10.
- [9] Ryu Ishizaki et al. “A Thermal Dynamic SOC Estimator for Lithium-Ion Batteries”. English. In: IEEE, 2015, pp. 1–6.
- [10] Naoki Kawarabayashi et al. “A Battery Smart Sensor and Its SOC Estimation Function for Assembled Lithium-Ion Batteries”. In: ().
- [11] I. Aizpuru et al. “Passive balancing design for Li-ion battery packs based on single cell experimental tests for a CCCV charging mode”. English. In: IEEE, 2013, pp. 93–98. ISBN: 9781467344296;146734429X;

- [12] TJ Barlow et al. “A reference book of driving cycles for use in the measurement of road vehicle emissions”. In: *TRL Published Project Report* (2009).
- [13] M. Broussely et al. “Main aging mechanisms in Li ion batteries”. English. In: *Journal of Power Sources* 146.1 (2005), pp. 90–96.
- [14] J. Vetter et al. “Ageing mechanisms in lithium-ion batteries”. English. In: *Journal of Power Sources* 147.1 (2005), pp. 269–281.
- [15] Guy Sarre, Philippe Blanchard, and Michel Broussely. “Aging of lithium-ion batteries”. English. In: *Journal of Power Sources* 127.1 (2004), pp. 65–71.